Investigating and Identifying the Electroreduction Pathways of Carbon Dioxide via Enhanced Vibrational Spectroscopy

Undergraduate Research Thesis

Presented in partial fulfillment of requirements for graduation with *research distinction* in Chemistry in the undergraduate college of The Ohio State University

by

Chibuokem Amuneke-Nze

The Ohio State University

May 2013

Project Advisor: Assistant Professor Anne Co, Department of Chemistry and Biochemistry

Abstract

As the world's energy needs continue to rise, and our conventional resources are depleted it is becoming increasingly clear that the current methods used to meet our societal demands, are not sustainable. The development of renewable energy technology will be essential to make a significant contribution to the future stability of our society's environmental and material health. Thus, the utilization of industrially and naturally abundant resources such as solar energy and carbon dioxide (CO_2) are increasingly attractive. Electrochemical reduction is a promising method for converting CO_2 to useful, high energy density chemical compounds and feed stocks. Product distribution from the reduction of CO_2 greatly depends on the electrolyte composition, preparation of the catalysts and reduction potential. This project examines the electrochemical pathways of CO_2 reduction by detecting the reaction intermediates on copper-based catalysts. By employing in-situ Raman spectroscopy on multifunctional Surface Enhancing Raman Scattering (SERS) materials this investigation aims to advance our understanding of CO_2 reduction and improve the efficacy of its heterogeneous catalysis. Here we report our attempts for fabricating patterned copper and gold materials and our systematic optimization of nanoporous copper SERS catalyst. In addition, we present the initial data on the in-situ detection of reaction intermediates on our substrates, produced during CO_2 electro-reduction to various chemical compounds.

Table of contents

1.1 Climate Change: Carbon Dioxide and the Environment

Since the First Assessment Report of the Intergovernmental Panel on Climate Change (IPCC) in 1990, governments have attempted to assess the validity and conditions related to climate change [1]. There are several aspects that link climate change with the development of societies and increases in greenhouse gases (GHGs) like carbon dioxide (CO_2) [2,3]. Their report investigates many possible links in depth and illustrates where climate change and sustainable development are mutually progressing. "Climate Change 2007 – Mitigation", the volume of the Assessment Report of the IPCC, provides a detailed analysis of the detriments and benefits of different approaches to mitigating and avoiding the effects of climate change [4]. The IPCC defines climate change as a change in the state of the climate that can be identified by scientific and statistical tests, via observing variations in the mean of its properties, and the properties that persists for an extended period, typically decades or longer [5,6]. Any change in climate over time, whether due to natural variability or as a result of human activity, provides clarity and understanding to policy makers and communities around the globe about what can be done to reduce or avoid climate change [7]. How much time is available to realize the drastic reductions needed to stabilize greenhouse gas concentrations in the atmosphere? What technologies must be utilized for mitigation? What is the benchmark for the adaptation to future GHG emission/radiative forcing trajectories? How can climate mitigation policy be aligned with sustainable development policies [8,9]? In order to answer these questions the IPCC and United Nations Framework Convention on Climate

Change (UNFCCC) have identified different factors that can contribute to the statistics that are observed in relation to climate change [10]. The natural interference or the common variability in climate in the environment and the anthropogenic interference referring to the variability due to human activity, are two terms used as conclusive markers to distinguish the results of change. The main human contribution to the change is the net emission carbon dioxide (CO_2). Some of the most popular or more publically recognized traits of climate change have been the changes in sea level and the rise in average temperature changes. The latter, average temperature increases are observed worldwide, with great prevalence at higher northern latitudes (Figure 1) [11].

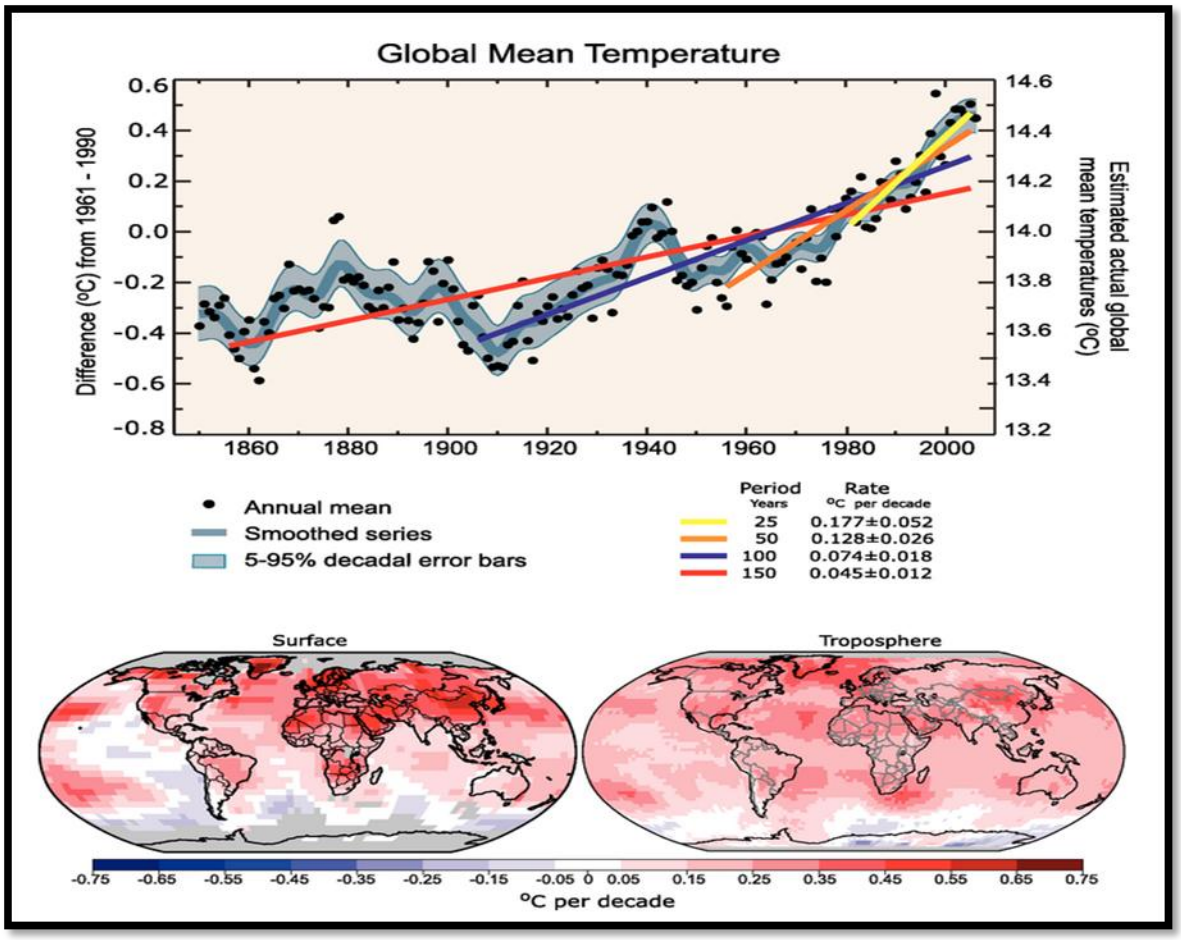

Figure 1: Observed changes in global average surface and atmosphere temperature. [11]

Interestingly, the mean Arctic temperatures have increased at close to double the global average. The annual mean temperature has increased dramatically from 1950 to 2010. While the rate of decadal warmth is consistently trending upwards, with century long degrees Celsius rate (°C rate) trends showing less drastic increases while, the half and quarter century rates display a distinct shift upwards from previous measurements. For example, from 1960-2010 the half century °C rate is nearly three times that of the 150 year rate while the 25 year rate is nearly 4 times the rate as measured from 1860 to 2010 and over twice the rate of the 1910 rate of decadal temperature increase. The staggering

aspect revealed here is the consistent increase in the rate of warming, from over a century in the past, till now. The trend observed is most likely due to our developing societies increasing industrial progression and dependence to meet our communal needs. As can possibly be inferred from Figure 1, the decadal rate most relevant to our present circumstances is the 25 year long measurement, since it reveals the most applicable observations of the warming occurring now. Also, the rates, when considered together, show that as populations and economies continue to grow and progress, as they have done over the years, the extent of the warming rate will most likely increase proportionally. Thus, the degree of their effects will become more prominent and the alleviation or sustainable equilibration of the environment will most likely become more and more difficult to achieve with every passing decade. This could lead to a situation where it will become less likely to integrate more environmentally conscious methods into a growing community's infrastructure, due to each economy's continued increase of their respective production and energy demands [12]. The other publically recognized aspect or direct effect of climate change, other than surface warming, is a rise in sea level. There is actually a strong correlation with sea levels and warming of the globe, the increases in sea levels observed are consistent with the rising temperature (Figure 2) [13]. The global average sea level rose at a rate of 1.3 to 2.3 mm/year from 1960 to 2000 and from 1993 to 2003 at a rate of 2.4 to 3.8 mm/year.

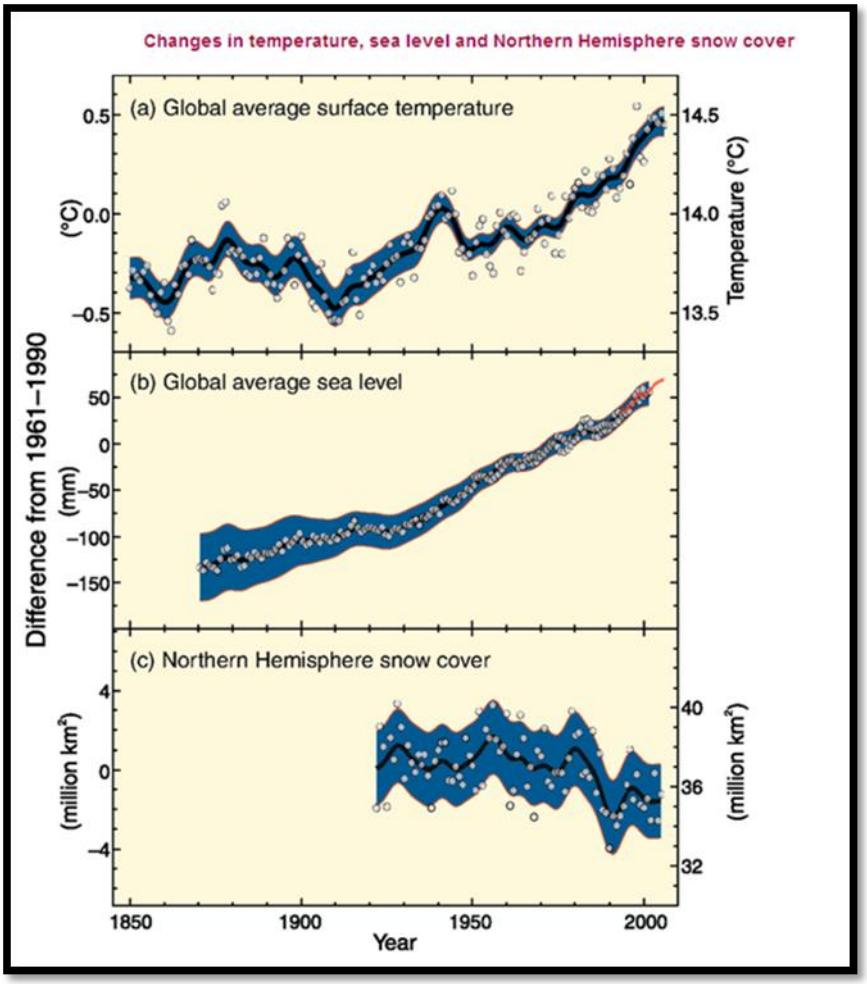

Figure 2: Observed changes in (a) global average surface temperature; (b) global average sea level from tide gauge (blue) and satellite (red) data; and (c) Northern Hemisphere snow cover for March-April. All differences are relative to corresponding averages for the period 1961-1990. Smoothed curves represent decadal averaged values while circles show yearly values. The shaded areas are the uncertainty intervals estimated from a comprehensive analysis of known uncertainties (a and b) and from the time series [13]

However, whether the faster rate of escalating sea levels in the shorter-term trend is due solely to the thermal expansion of oceans alone is often debated. Though, many agree that it is most likely the dominating factor with some other lesser factors that contribute to the sea level trends observed. One possible supporting observation to this conclusion is the observed decreases in ice and snow prevalence that are consistent with the rising sea level and global warming. Since the early 1900s until now, maximum areal extent of seasonally frozen surface has decreased by 7% [14]. Some possible observations and

effects as a result of this climate change may lead to extreme weather events in the future, and may be a factor involved with the changing frequency in both seasonal and unseasonal periods in the last 50 years. It is likely that frosting and cold days and nights have decreased in frequency over most land regions while heat waves, along with hot days and nights, have increased in frequency. Also, it is quite possible the rises in sea level have become more frequent in a wide range of areas worldwide due to climate change. The assessment concludes that there is high confidence that the observed changes globally and regionally are due to warming and may have an impact on physical and biological systems [15]. There are also effects of temperature increases reported with medium confidence such as forestry and agriculture disturbances along with increased human health cases and seasonal pollen/ allergenic agents. In addition, warming of rivers and lakes in multiple regions affecting water quality and strongly affecting terrestrial biological systems are noted to show strong correlation to the warming. The extent of the warming has multiple effects on the environment and society. However, as mentioned earlier, the main drivers of the change must be identified and taken into account if mitigation is to be set in place. Both the anthropogenic and natural causes of climate change such as, radiative forcing, greenhouse gas (GHG) emissions and their atmospheric concentrations are of concern when distinguishing the source of the change [16]. GHG emissions due to the anthropogenic effect or as a result of human activity have increased an estimated 70% since the modern preindustrial era 1970-2004 (Figure 3A). Carbon dioxide (CO_2) is the most predominant anthropogenic GHG. The radiative forcing of the environment system is largely influenced by long lived GHGs like CO_2 (Figure 3B) [17]. Radiative forcing (RF) is a measure of the extent of influence a factor, such as carbon

dioxide (CO_2), methane (CH4), nitrous oxide (N2O), or hydrofluorocarbons /F-gases (H/PFCs), has in altering the balance of incoming and outgoing energy in the Earth-atmosphere system. Also it is an index of importance, which reveals different factors and their potential climate change contribution mechanism. RF is expressed in watts per square meter (W/m2). For reference "Gt CO_2 eq/yr" stands for the units of total annual emissions of greenhouse gases and particles in equivalent carbon dioxide units, gigatonnes (Gt).

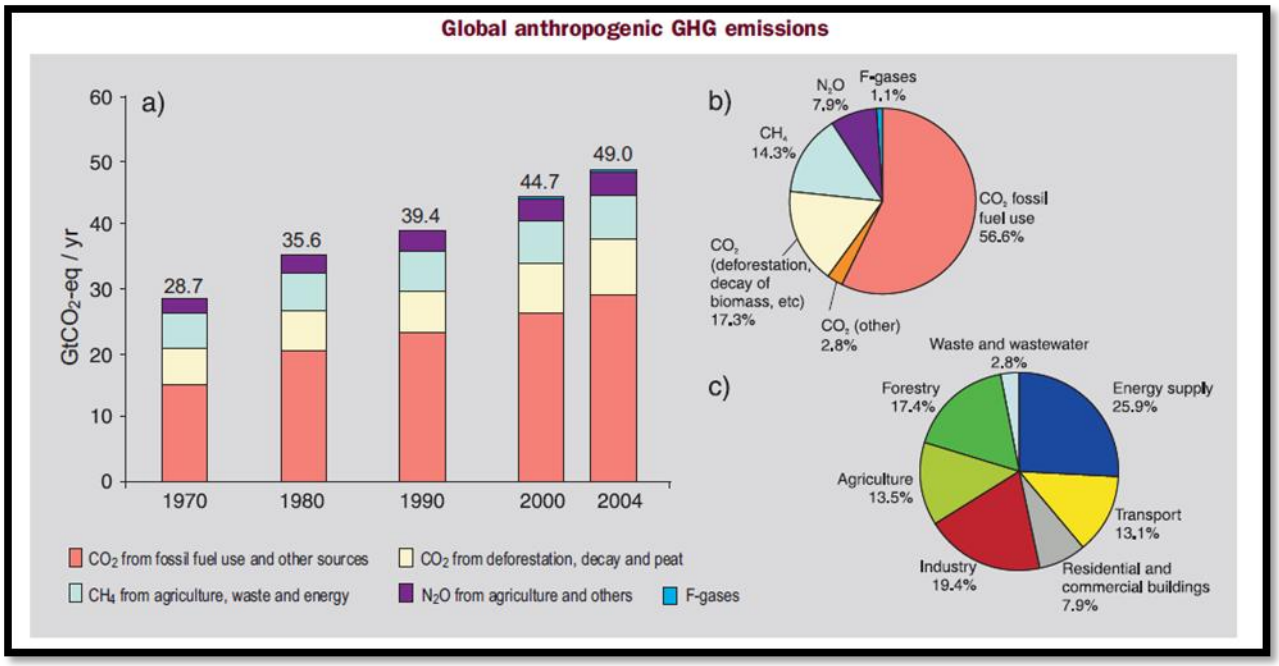

Figure 3A: (a) Global annual emissions of anthropogenic GHGs from 1970 to 2004. (b) Share of different anthropogenic GHGs in total emissions in 2004 in terms of CO2-eq. (c) Share of different sectors in total anthropogenic GHG emissions in 2004 in terms of CO2-eq. "Gt CO_2 eq/yr" stands for the units of total annual emissions of greenhouse gases and particles in equivalent carbon dioxide units [17]

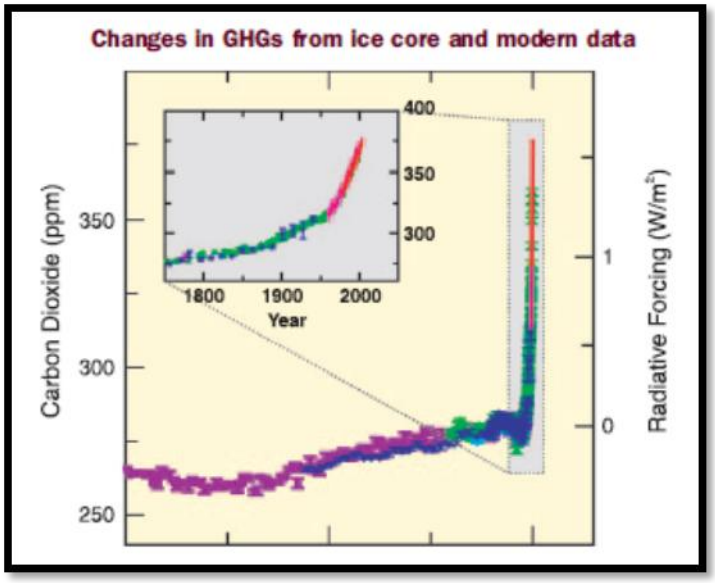

Figure 3B: Global annual Radiative Forcing for Carbon Dioxide [18]

Particles equivalent to carbon dioxide CO_2 annual emissions rose from 21 to 38 Gt from 1970 to 2004 and represented 77% of total emission in 2004, and over 55% due to anthropogenic fossil fuel emissions. The rate of emission is much higher in the 4 year period 2000 to 2004 (1.07 $GtCO_2$-eq/yr) than during previous periods observed, 1970-1980 (0.70 $GtCO_2$-eq/yr) 1980-1990 (0.39 $GtCO_2$-eq/yr) 1990-2000 (0.55 $GtCO_2$-eq/yr) [18]. In addition, the 4 year period rise in anthropogenic fossil fuel emissions nearly matches each 10 year period increases with an average of double their respective rates. This recent trending is expected to continue as nations develop and populations increase. It's worth mentioning that the largest contribution to the rising GHG has come from the energy supply, industry and transport sectors. While, it has been observed that agriculture, residential buildings and forestry have anthropogenic contributions that rise at a much lower rate. Global increases in CO_2- levels rose from 280 ppm 1970 to 379 ppm in 2004, generally the increases are due to an inadequate removal process. In conjunction, warming due to the increased emission reduces the fraction of CO_2 ocean

uptake, thus increasing the portion of anthropogenic emission remaining in the atmosphere. This can possibly results in a partial positive carbon feedback where larger long lived GHGs induce more severe climate change effects due to anthropogenic CO_2 reaching dangerous levels. Thus preventing dangerous levels of anthropogenic interference in the climate requires adaptation of our energy supply infrastructure and defined mitigation in response to the change. However, both involve an iterative or a developmental risk management process that includes both mitigation and adaptation. When responding to the climate change, taking into account the actual and avoided climate change damages, co-benefits, sustainability, equity and attitudes to risk is necessary. Climate change impacts depend on the characteristics of natural and human systems, their developmental pathways and their specific locations [19]. This must be understood to prevent dangerous anthropogenic interference levels with the climate system and achieve a constructive level (Figure 4) [20].

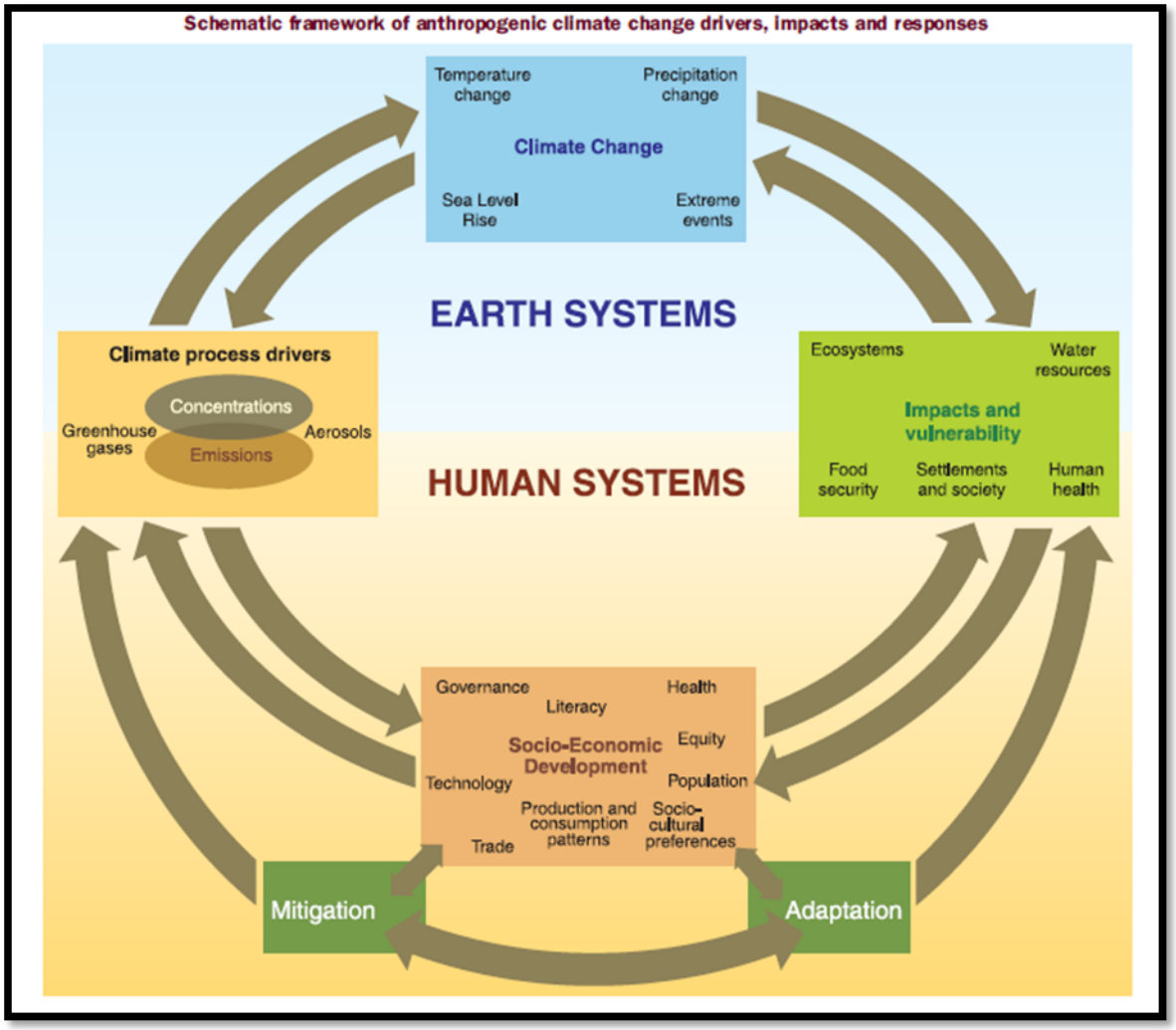

Figure 4: Diagrams of the relationships between climate change, the anthropogenic, and natural factors [20]

Important vulnerabilities may be associated with many "climate-sensitive" systems, such as effects on energy infrastructure, food supply, health, water resources, coastal systems, ecosystems and global biogeochemical cycles. The equilibrium climate sensitivity is a degree of the climate system response to sustained radiative forcing [21]. It is imperative that such an equilibrium level should be achieved within a sufficient time frame to allow ecosystems to adapt naturally to climate change, to ensure that ecosystems and food production are not threatened and to enable economic development to proceed in a

sustainable manner. On a global scale, regional aspects are often a difficult variable. There are distinct differences across regions and those in a weaker economic position are often the more vulnerable to climate change and are frequently the most susceptible to climate-related damages, especially when they face multiple stresses that aggravate their political and economic systems [22]. There is good evidence of greater vulnerability of specific groups, such as the poor and elderly, not only in developing but also in developed countries. There is greater confidence in the projected regional patterns of climate change and in the projections of regional impacts, enabling better identification of particularly vulnerable systems, sectors and regions. Knowing that adaptation is necessary, both in the short term and longer term, to address the impacts resulting from the warming that would occur even for the lowest stabilization levels; many novel processes and policies are required for sufficient progress. Adaptation and mitigation can complement each other; and, together can significantly reduce the risks of climate change with prudent techniques like CO_2 harnessing for energy supply and correct emission trajectories [23]. Drastic reductions in CO_2 emissions and the synthesis of non-fossil fuel energy sources are critical to minimize the effects of CO_2 as a GHG in the atmosphere and reduce our dependence on imported nonrenewable energy sources, most notably petrol chemicals. Recycling of CO_2 to an energy carrier, thereby reducing its accumulation in the atmosphere and inducing the production of renewable fuels from CO_2, water, and renewable electricity for use as transportation fuels is a prudent notion. Also the method presents a convenient means of storing electrical energy in a chemical form to level the electrical output from present intermittent energy sources such as wind and solar.

1.2 Carbon dioxide and Industry Specific Energy Consumption

The detrimental effect of climate change is strongly related to GHG and our energy consumption. The annual total greenhouse gas (GHG) emissions due to the global energy supply sector continue to rise. Combustion of fossil fuels continues to dominate the worldwide energy market that attempts to meet the ever-increasing demand for heat, electricity and transport fuels. GHG emissions from fossil fuels have increased each year as noted in the IPCC 2001 Third Assessment Report (TAR) (IPCC,2001), despite greater deployment of low- carbon technologies; for instance, the utilization of renewable energy and their implementation has been hindered [24]. Without the near-term introduction of supportive and effective policy actions by governments, energy related GHG emissions, mainly from fossil fuel combustion, are projected to rise by over 50% from 26.1 GtCO2eq (7.1 GtC) in 2004 to 37–40 GtCO2 (10.1–10.9 GtC) by 2030. Mitigation has therefore become even more challenging. Global dependence on fossil fuels has led to the release of over 1100 GtCO2 into the atmosphere since the mid-19th century. Currently, energy-related GHG emissions, mainly from fossil fuel combustion for heat supply, electricity generation and transport, account for around 70% of total emissions including carbon dioxide, methane and some traces of nitrous oxide and F-gases [26]. To continue to extract and combust the world's rich endowment of oil, coal, and natural gas at our current or increasing rates, and so release more of the stored carbon into the atmosphere, is no longer environmentally sustainable, unless carbon dioxide capture, storage, and harnessing (CCSH) technologies currently being developed can be synthesized and

widely deployed. Then the regional and societal variations in the demand for energy services and environmental effects may be appeased.

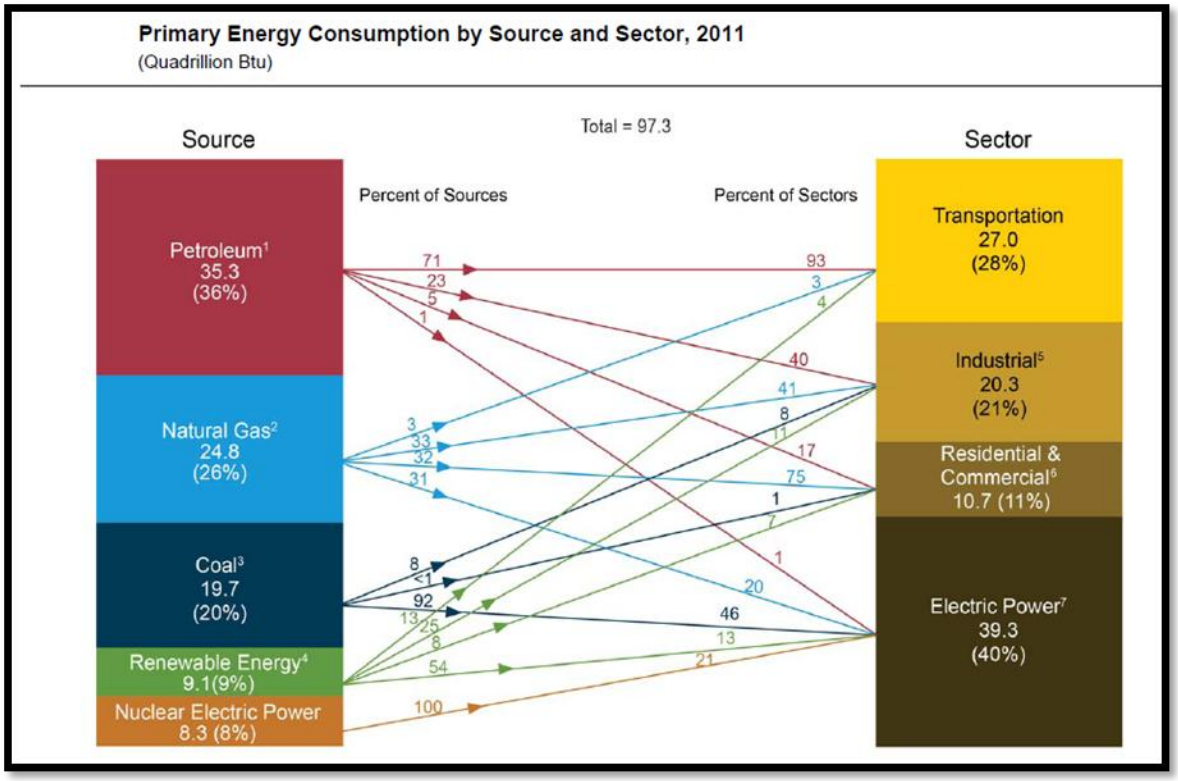

Figure 5: (a) Types of energy consumption by sector [26]

Energy access, equity and sustainable development are compromised by higher and rapidly fluctuating prices of petroleum resources like oil and gas, which dominated the energy supplies utilized by the four main sectors (Figure 5). These factors increase the incentives to deploy carbon-free and low-carbon energy technologies, due to the market uptake of coal, cheaper unconventional hydrocarbons and technologies with consequent increases in carbon dioxide (CO_2) emissions. Increasing renewable energy access for all will require making available basic and affordable energy services using a range of energy resources and innovative conversion technologies while minimizing GHG emissions, adverse effects on human health, and other local and regional environmental

impacts. To accomplish this, it would require governments, the global energy industry and society as a whole to collaborate on an unprecedented scale. At present, the industrial and transportation sectors dominate energy consumption (Figure 6) [27]. The method used to achieve optimum integration of heating, cooling, electricity and transport fuel provision with more efficient energy systems will vary with the region, local growth rate of energy demand, existing infrastructure and implementation benefits.

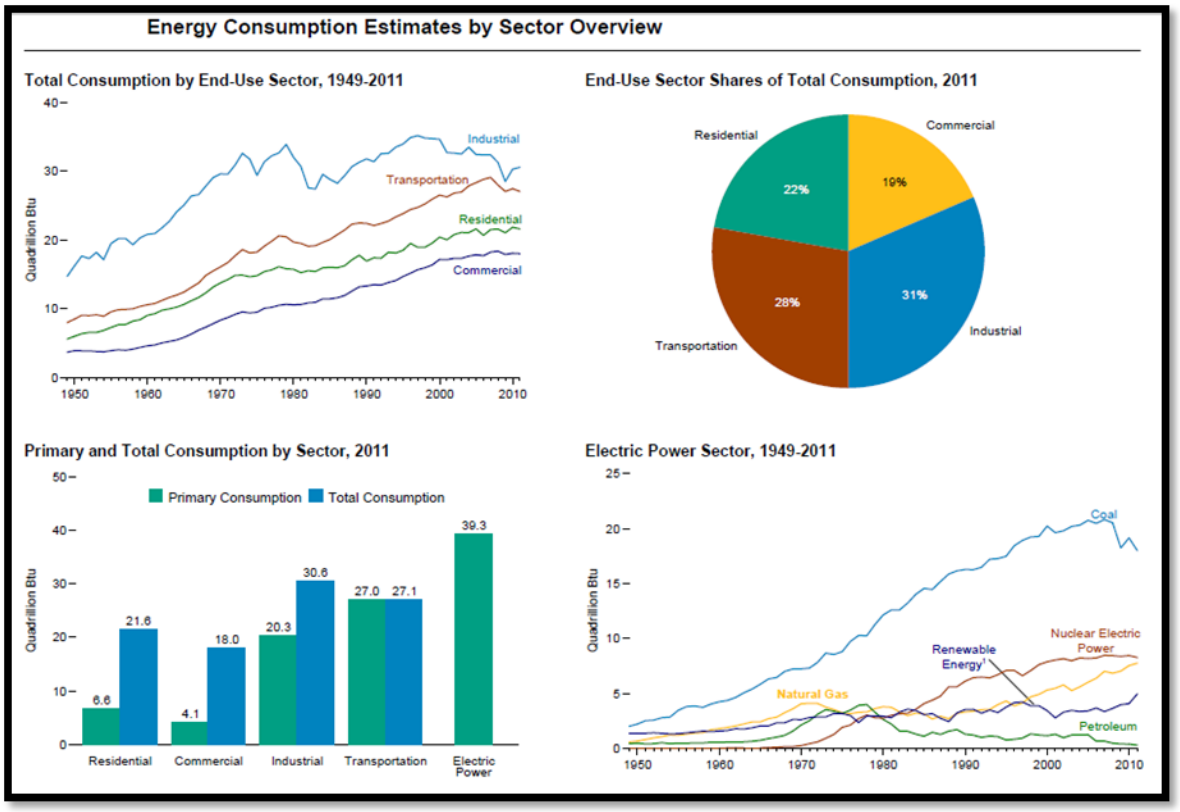

Figure 6: Energy consumption by sector [27]

The wide range of energy sources and carriers that provide energy services need to offer long-term security of supply, be affordable and have minimal impact on the environment. However, these three public objectives often compete, at present there are "sufficient" reserves of most types of energy resources to possibly last several decades at current rates

of use when using technologies with efficient energy-conversion designs. How best to use these resources in an environmentally acceptable manner while providing for the needs of growing populations and developing economies is one of the greatest challenges opposing our populace.

1.3 Future Energy Supply Contribution and Renewable Energy Role

Conventional oil reserves will eventually peak as will natural gas reserves, but it is unclear exactly when and what the nature of the transition to alternative fuels will look like after its climax and the rising energy demands [28]. It is still uncertain how and to what extent alternatives will reach the mainstream market and its sectors and then what the resultant changes in global GHG emissions trajectories and RFs will be as a result. Conventional natural gas reserves are more abundant in terms of energy than conventional oil, but they are also distributed less evenly across regions [29]. Unconventional gas resources are also abundant, but future economic development of these resources is unclear. For instance, coal is irregularly distributed, but remains abundant. It can be converted to liquids, gases, heat and power, although more intense utilization will increase demand for viable CCSH technologies if GHG emissions from its use are to be limited [30,31]. For instance, to reduce dependence on imported petroleum the expansion of coal to liquid (CTL) technology has been suggested. CTL produces syngas, a combination of CO and hydrogen gas, which can then be further processed into fuels via Fischer-Tropsch process [32,33]. However, it requires subsequent CCSH implementation to decrease emissions of CTL technologies use as transportation fuels; but this solution does not address the nonrenewable characteristics of the fossil fuel. There is a trend towards using energy carriers with increased efficiency and convenience, particularly toward liquid fuels and electricity, while away from solid fuels. Nuclear energy, already over 8% of total primary energy, could make an increasing contribution

to carbon-free electricity and heat in the future. Another potentially sustainable alternative to fossil fuels being investigated are the production of biofuels from algae and woody biomass [34]. Traditional biomass for domestic heating and cooking still accounts for more than 10% of global energy supplies but could eventually be replaced, mainly by modern biomass and other novel energy systems which utilize biomass most effectively. These are encouraging technologies that could potentially supply carbon neutral fuels while minimizing competition with the food supply. Wind, solar, and tidal power are also very popular and expanding rapidly along with increased interest in expanding nuclear energy [35]. A very attractive alternative to CO_2 sequestration, CCSH is the use of captured carbon as a reagent for producing useful chemicals either through chemical or electrochemical means. The crucial goal taken into account is that the electricity used to supply the CO_2 conversion must be renewable, or at least from a carbon-neutral source such as a nuclear reactor; otherwise, increased CO_2 would be emitted in producing the electricity than would be reduced in the process. In addition, the storage of electrical energy in chemical form is potentially useful in two key areas, leveling the output from intermittent electricity sources, such as wind and solar, and allowing increased utilization. Several major barriers of renewable technologies are: economics, proliferation, long-term fuel resource constraints, security, stability, waste management, and adverse public opinion [36]. Renewable energy sources are widely dispersed and have better recycling prospects compared to fossil fuels, which are concentrated at individual locations and requiring distribution. Thus, renewable energy must either be utilized via a distributed manner or concentrated to meet the higher energy demands of cities and industries. Other renewable energy-supply technologies mentioned before, particularly solar, wind,

geothermal and biomass, are currently small overall contributors to global heat and electricity supply, but are the most rapidly increasing technologies [37]. Costs, as well as social and environmental barriers, are also restricting the growth of most of the non-conventional energy sources. Therefore, increased rates of deployment will likely need supportive government measures to progress forward. Currently our consumption of petrol chemicals dominate the transportation and industrial sectors, contributing nearly 35 Quadrillion Btu in 2010 (Figure 7) [38]. While electric energy alone contributes a much lesser faction.

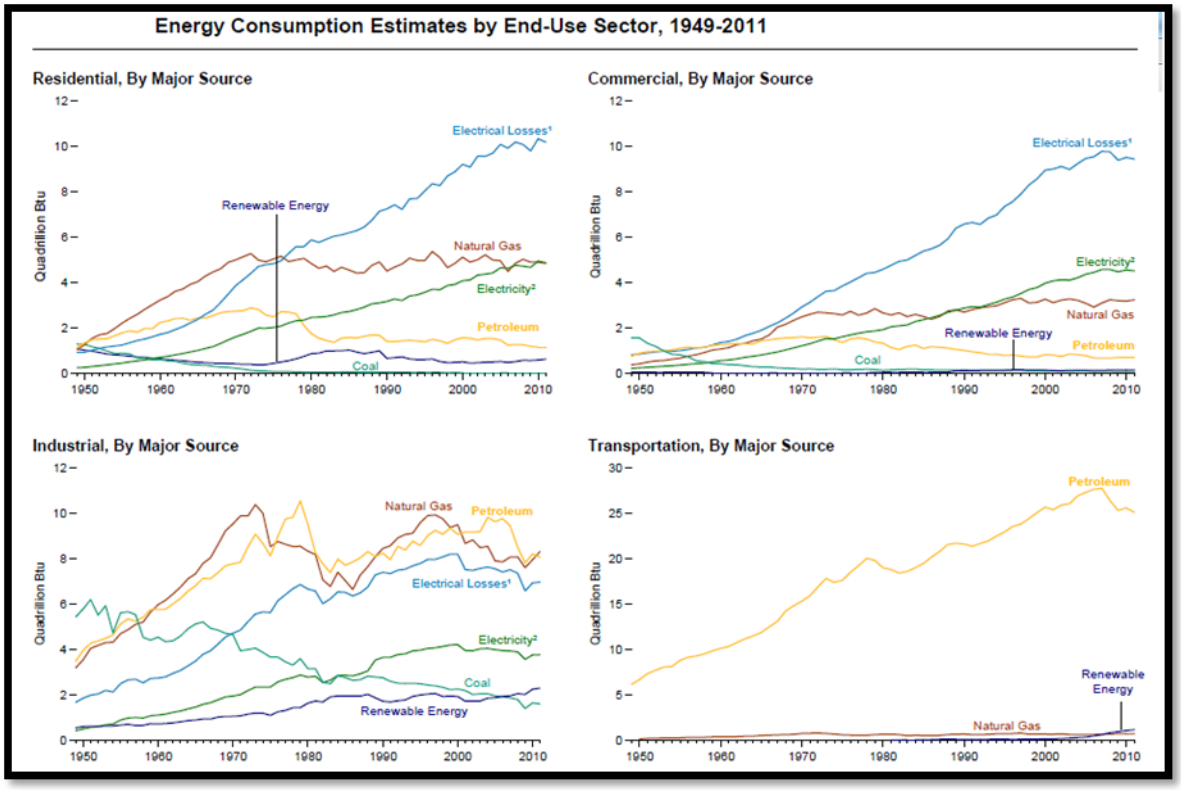

Figure 7: Energy distribution by sector [38]

Security of energy supply issues and perceived future benefits from strategic investments should encourage the greater uptake of lower carbon-emitting technologies but our

cultural standards are often the critical obstacle. The numerous worries about the future security of conventional oil and gas supplies could aid the transition to more low-carbon technologies such as nuclear, renewables and CCSH. However, the development of usable and practical materials and processes for CCSH is a determining factor. As a result, studies in these new areas of energy production must be done. Addressing environmental impacts predominantly depends upon the introduction of large-scale renewable energy-conversion plants, government regulations, and/or tax incentives rather than depending on market mechanisms [39]. Thus, decisions taken today that support the deployment of carbon-neutral technologies, especially in countries seeking supply security to provide sustainable development paths, could have profound effects on GHG emissions for the next several decades. Smaller-scale, distributed energy plants using local energy resources and lower to zero-carbon emitting technologies, can give added reliability, be built more quickly and be efficient by utilizing both heat and power outputs locally. Integrating electrical systems could help reduce transmission losses and more energy-efficient technologies can also improve supply security by reducing future energy-supply demands and any associated GHG emissions. The transition from surplus fossil fuel resources to constrained gas and oil carriers, and subsequently to new energy supply and conversion technologies, has begun. However, it faces regulatory barriers to rapid implementation; and, market competition alone may not lead to reduced GHG emissions [40]. Nevertheless, the energy systems of many nations are evolving from their historic dependence on fossil fuels in response to the climate change threat, market failure of the supply chain, and increasing reliance on global energy markets; thereby necessitating the wiser use of energy in all sectors. A rapid transition toward new energy

supply systems with reduced carbon will require management to minimize economic, social and technological risks and to draft stakeholders who retain strong interests in maintaining the unsustainable status quo. System advancements for stabilization levels are assessed to have a higher probability to be achieved by deployment of a collection of technologies that are either currently available or expected to be commercialized in coming decades, assuming related barriers are broken down. Worldwide deployment of low-GHG emission technologies, as well as technology improvements, research, and development, in the public and private sectors would be a necessity for achieving equilibrium targets as well as cost agreements. The contribution of different technologies varies over time and region, and depends on the standard development and analysis available technologically, and their respective costs. Stabilization at the lower of the assessed levels of 490 to 540ppm CO2-eq requires early substantially increased diffusion of advanced low-emissions and CCSH technologies over the next decades (2000-2030). Most assume that increased contributions across abatement options in the long term require that the barriers to development, acquisition, deployment and diffusion of technologies are effectively addressed with appropriate mitigation and adaptation to achieve emission reduction at a significant scale. There are multiple uncertainties concerning the future contribution of different technologies. However, all assessed stabilization scenarios concur that 60 to 80% of the reductions over the course of the century would come from energy supply and use and industrial processes, including non-CO_2 and CO_2 land-use and forestry mitigation options which provides greater flexibility and cost-effectiveness. Energy efficiency plays a key role across many scenarios for most regions and time scales. For lower stabilization levels, scenarios put more emphasis on

the use of low-carbon energy sources, such as renewable energy, nuclear power and the use of

CCSH.

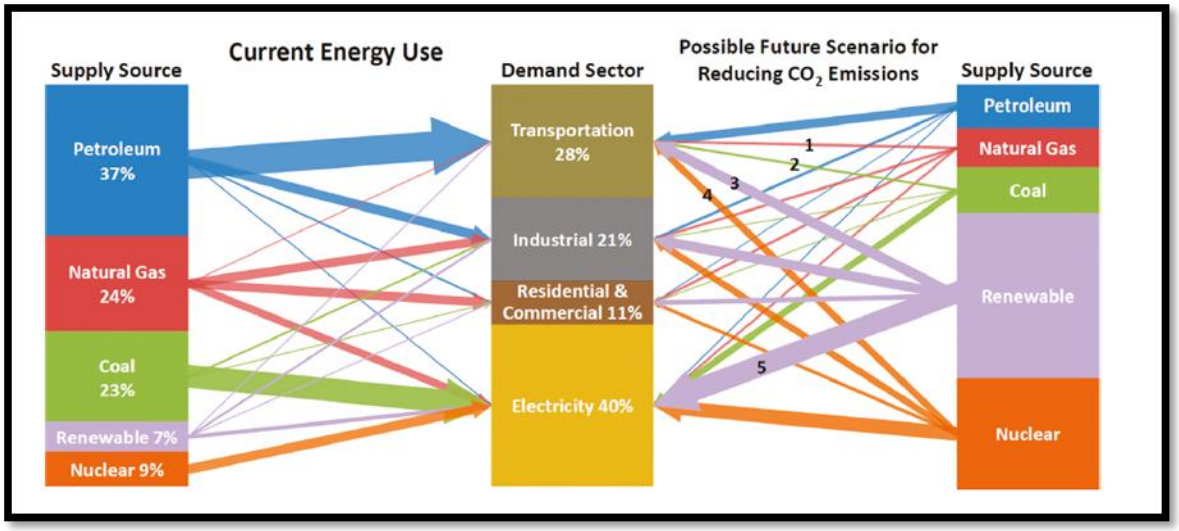

Figure 8: (a) Primary U.S. energy consumption by source and sector for 2008 (left) compared to a hypothetical, qualitative scenario in which emissions are reduced by significantly reducing fossil fuel consumption (right). Key enabling technologies in the future scenario are (1) gas to liquid conversion, (2) coal to liquid conversion, (3) biofuels and electrochemical conversion of CO_2 to liquid fuels using renewable electricity, for example, wind and solar, (4) electrochemical conversion of CO_2 to liquid fuels using electricity from nuclear power, and (5) wind, solar, and tidal power with storage via electrochemical conversion of CO_2 or other methods such as pumped hydro, compressedair, and flow batteries [41]

A myriad of studies have shown that significant reductions in CO_2 emissions are required to limit the potential effects of climate change. The fact that fossil fuel consumption accounts for the bulk of CO_2 emissions and the push to reduce dependence on imported fossil fuels, indicates that drastic reductions of fossil fuel use will be needed in the future, even with increases in the energy demand. The potential role of renewable, nuclear and CCSH energy sources is displayed in (Fig 8) [41]. It notes a few of the challenges that such changes would set forth and the possible contributions that the novel technologies could take on by comparing our present energy consumption with a hypothetical situation in which fossil fuel use is significantly reduced as part of the efforts to reduce CO_2 emissions and dependence on unsustainable energies. This information reveals several

key aspects of our current energy use in relation to its sources. The most significant aspect is the nearly complete dependence of the transportation sector on petroleum-derived liquid fuels. Similarly, the vast majority of carbon-neutral energy and renewables produce electricity, effectively limiting the utilization of these desirable energy sources to the electrical grid. Even though it is just a hypothetical display, the reductions could be achieved in many different ways, depending on which technologies are most feasible and end up being implemented at a meaningful scale [42]. This will hinge upon factors like local environment, economic conditions, and the technical merit of each technological process.

As fossil fuels dominate the energy portfolio and concerns over climate change rise, the challenges that will be faced in meeting energy demands of the future can be overcome by employing new energy resources that supplant our major element, namely petroleum combustion. While the exact construct and distribution of future energy supply sources may be uncertain, undoubtedly, we will need to move from fossil fuels to sustainable energy. The leading challenge, will involve continuing to supply the transportation sector while fossil fuel use is being phased out. Since it is unlikely that a complete overhaul to hydrogen fuel cell, CTL syngas, or battery powered vehicles is made, liquid-hydrocarbon fuels will continue to play a role until their depletion. One proposal could be CO_2 conversion and storage in a chemical form via the electrochemical reduction of CO_2 gives added versatility as the products can be used as sources for electricity production, transportation fuels, or chemical feedstocks. These two concepts, the need to continue to provide energy to the transportation sector and the need to increase electricity contribution from carbon neutral sources, mark the value of a process that could renovate

and thus store electrical energy in a chemical form, both for facilitating the penetration of renewable energy into sectors such as transportation and for storing excess electricity.

1.4 Electroreduction of CO_2

As previously discussed, the prominent presence of CO_2 in the atmosphere is a plight that our society has faced and continues to encounter today. The electroreduction of CO_2 has been studied by scientist as early Volta. However, more recently, professor Hori worked extensively on understanding the potential role of CO_2 as a carbon resource, when using chemical fixation. Hori theorized heterogeneous conversion of carbon dioxide via electrochemical methods would be scalable to address CO_2 utilization and recycling [43]. Since CO_2 is one of the most stable carbon based substances in environmental conditions its incorporation into industrial resources has been minimal or slowly increasing. Its chemical reactivity is low but the equilibrium potentials are not very negative compared to hydrogen evolution reaction in aqueous electrolyte solutions. Standard electrode potentials of CO_2 reduction to products are shown below for the formation of carbon monoxide (CO), methane (CH_4), ethylene (C_2H_4), ethanol (C_2H_5OH), and propanol (C_3H_7OH) (Fig 9A).

1) $CO_2 + H_2O + 2e^- = CO + 2OH^-$ (–0.52 V)

2) $CO_2 + 6H_2O + 8e^- = CH_4 + 8OH^-$ (–0.25 V)

3) $2CO_2 + 8H_2O + 12e^- = C_2H_4 + 12OH^-$ (–0.34 V)

4) $2CO_2 + 9H_2O + 12e^- = C_2H_5OH + 12OH^-$ (–0.33 V)

5) $3CO_2 + 13H_2O + 18e^- = C_3H_7OH + 18OH^-$ (–0.32 V)

Figure 9A: Standard reduction potentials based on thermodynamic data at pH 7.0. [43]

Hori has extensively investigated CO_2 electrochemical reduction on various metal electrodes such as Lead (Pb), Tin (Sn), Gold (Au), Silver (Ag), Zinc (Zn), Copper (Cu), and Nickel (Ni). The metals each produce a multitude of products when employed as electrodes under mild conditions with varying faradaic efficiency (Fig 9B). For instance Sn when held at a current density of 5.0mA/cm^2 applying a potential of -1.63V vs. a standard hydrogen electrode (SHE) produces CO, hydrogen (H_2), and formate ($HCOO^-$) at efficiencies of 7.1%, 4.6% and 88.4% respectively. These percentages add up to over 100% due to the reaction of H_2O in the solvent.

Table 3
Faradaic Efficiencies of Products in CO_2 Reduction at Various Metal Electrodes. Electrolyte: 0.1 M $KHCO_3$, T = 18.5 ± 0.5°C. Reprinted from Ref. 23, Copyright (1994) with Permission from Elsevier

Electrode	Potential vs. SHE V	Current density mA cm^{-2}	Faradaic efficiency, %							
			CH_4	C_2H_4	EtOH[a]	PrOH[b]	CO	$HCOO^-$	H_2	Total
Pb	−1.63	5.0	0.0	0.0	0.0	0.0	0.0	97.4	5.0	102.4
Hg	−1.51	0.5	0.0	0.0	0.0	0.0	0.0	99.5	0.0	99.5
Tl	−1.60	5.0	0.0	0.0	0.0	0.0	0.0	95.1	6.2	101.3
In	−1.55	5.0	0.0	0.0	0.0	0.0	2.1	94.9	3.3	100.3
Sn	−1.48	5.0	0.0	0.0	0.0	0.0	7.1	88.4	4.6	100.1
Cd	−1.63	5.0	1.3	0.0	0.0	0.0	13.9	78.4	9.4	103.0
Bi[c]	−1.56	1.2	-	-	-	-	-	77	-	-
Au	−1.14	5.0	0.0	0.0	0.0	0.0	87.1	0.7	10.2	98.0
Ag	−1.37	5.0	0.0	0.0	0.0	0.0	81.5	0.8	12.4	94.6
Zn	−1.54	5.0	0.0	0.0	0.0	0.0	79.4	6.1	9.9	95.4
Pd	−1.20	5.0	2.9	0.0	0.0	0.0	28.3	2.8	26.2	60.2
Ga	−1.24	5.0	0.0	0.0	0.0	0.0	23.2	0.0	79.0	102.0
Cu	−1.44	5.0	33.3	25.5	5.7	3.0	1.3	9.4	20.5	103.5[d]
Ni	−1.48	5.0	1.8	0.1	0.0	0.0	0.0	1.4	88.9	92.4[e]
Fe	−0.91	5.0	0.0	0.0	0.0	0.0	0.0	0.0	94.8	94.8
Pt	−1.07	5.0	0.0	0.0	0.0	0.0	0.0	0.1	95.7	95.8
Ti	−1.60	5.0	0.0	0.0	0.0	0.0	tr.	0.0	99.7	99.7

Figure 9B: (a) CO_2 reduction at various metal electrodes [43]

Also considering 2 other metals, Au and Cu, which produce products of CO, H_2 and $HCOO^-$ at efficiencies of 87.1%, .7%, 10.2% for Au held at -1.14V and 1.3%, 9.4%,

20.5% for Cu held at -1.44V vs. SHE. In addition, Cu produced other products such as CH_4, C_2H_4, C_2H_5OH, and C_3H_7OH at efficiencies of 33.3%, 25.5%, 5.7%, and 3.0%, respectively when held at a current density of 5.0 mA/cm^2. Understanding the data displayed led to the grouping of different CO_2 reduction metals by their respective major products (Fig 10) [44]. For example, CO_2 reduction on Cu electrodes resulted in mainly in hydrocarbon production. Other Cu alloys such as Cu-Ni, Cu-Cd, and Cu-Au produced hydrocarbons and display some versatility compared to other metals, like Pb and Ag, which are limited producing $HCOO^-$.

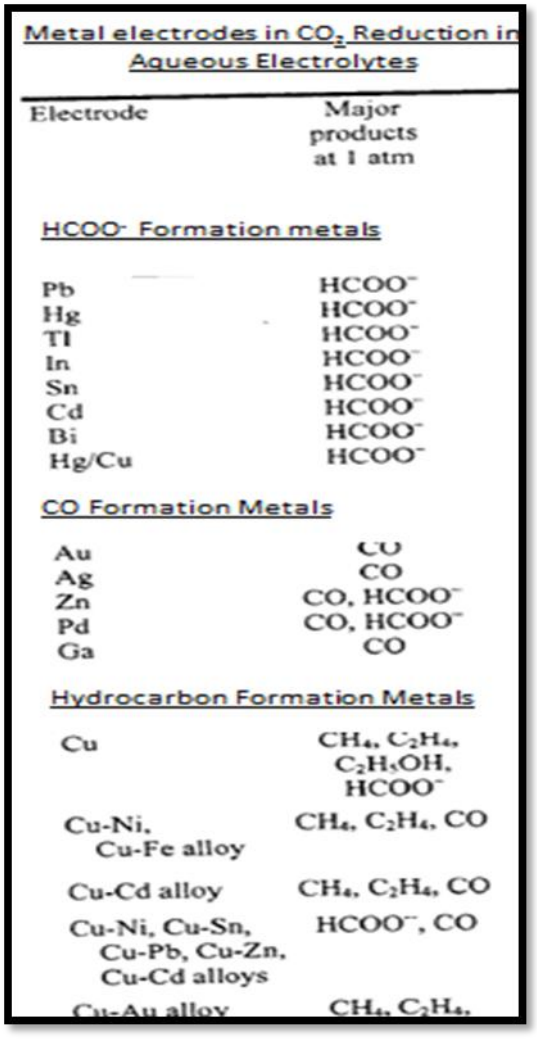

Metal electrodes in CO_2 Reduction in Aqueous Electrolytes

Electrode	Major products at 1 atm
$HCOO^-$ Formation metals	
Pb	$HCOO^-$
Hg	$HCOO^-$
Tl	$HCOO^-$
In	$HCOO^-$
Sn	$HCOO^-$
Cd	$HCOO^-$
Bi	$HCOO^-$
Hg/Cu	$HCOO^-$
CO Formation Metals	
Au	CO
Ag	CO
Zn	CO, $HCOO^-$
Pd	CO, $HCOO^-$
Ga	CO
Hydrocarbon Formation Metals	
Cu	CH_4, C_2H_4, C_2H_5OH, $HCOO^-$
Cu-Ni, Cu-Fe alloy	CH_4, C_2H_4, CO
Cu-Cd alloy	CH_4, C_2H_4, CO
Cu-Ni, Cu-Sn, Cu-Pb, Cu-Zn, Cu-Cd alloys	$HCOO^-$, CO
Cu-Au alloy	CH_4, C_2H_4,

Figure 10: CO_2 reduction at various metal/alloy electrodes grouping by major compound production [44]

Most CO_2 reduction experiments were obtained from electro-catalytic experiments done in aqueous solutions. However, CO_2 reduction in non-aqueous solutions can have significant improvements. One example, is the suppression of H_2 evolution which, in aqueous solution, normally competes with $HCOO^-$, hydrocarbon, or CO production due to the presence of excess water in solution. Also, the greater solubility of CO_2 in organic solvents can increase the overall conversion activity. His studies and several other groups have also shown the highly versatile characteristics of Cu electrodes for electro-reduction of CO_2. For instance in 2006 M. Gattrell , N. Gupta, and A. Co investigated electrochemical reduction of CO_2 to hydrocarbons on Cu electrodes to store and produce renewable energy (Fig 11) [45]. They displayed the product distribution of can be manipulated by the potential applied to the electrode. As noted, the initial work in this area focused on exploring different catalysts and the products that can be produced, as with Hori [46]. In addition, many more recent investigations have elucidated how parameters such as electrolyte and temperature favor certain products over others [47]. Investigators have shown how many parameters especially energy input can effect product distribution. Therefore, we need to know how intermediates are stabilized as a function of energy to infer a mechanistic pathway of the CO_2 reduction process. Thus research that aims to improve our understanding of CO_2 reduction reaction intermediates, will lead to more effective catalysts design [48].

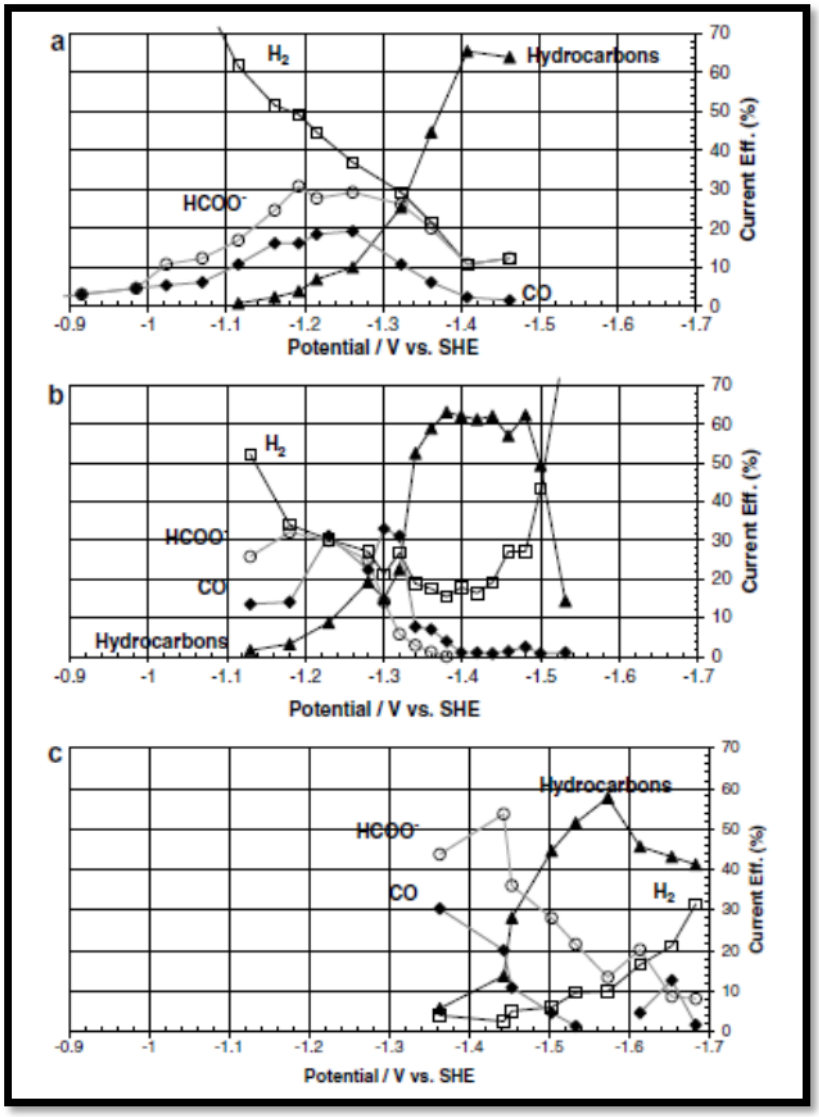

Figure 11: Current efficiencies at different potentials for CO2 reduction at copper electrodes. (a) 0.1M KHCO3, 1 atm CO2 bubbled, 19 _C (current range 0.12–7 mA/cm2), data from (b) 0.1M KHCO3, 1 atm CO2 bubbled, 25 _C, data from, (c) 0.1 M KHCO3, 30 atm CO2, stirred, 25 _C (current range 75–900 mA/cm2), data from.

The use of Cu electro-catalysis to synthesize fuels offers great potential in reaching carbon neutrality when with technologies such as photovoltaics, wind, or nuclear energy. Nevertheless, investigating how to improve the efficiency of the process, as is, with electrolytic reduction can also drive the implementation of CO_2 utilization. Altering factors and gaining a deeper understanding of the electrolyte and catalyst role in

conversion to decrease the overpotential required for conversion, increase electrode cycle stability, and current density may lead to the practical application of the process. Finally, the latest studies on the electrochemical reduction of CO_2 have shown the possibility of harnessing the potential of CO_2 as an energy store vector. Also, as a prospect for producing hydrocarbon fuels to mitigate unsustainable energy consumption and climate change issues.

1.5 Vibrational spectroscopy- Raman and SERS

Analytical techniques can be used to gain valuable information about chemical species, Raman spectroscopy is one type of these useful analytical tools. In the 1920s Chandrasekhara Venkata (C.V.) Raman, an Indian physicist, and colleagues were investigating optics with a focus on how light scattered; and, he discovered what is now called the Raman Effect. In his biography, it says he became intrigued by the question, 'Why is the sea, especially the Mediterranean Sea, so blue?' and he came to the conclusion that it is not due to reflected light from the blue sky but to scattering, in much the same way as the blue color of the sky is produced [49]. The scattering factor plays a dominant role, but to a small extent, the selective adsorption of water in the red and green also impacts the color. As Raman continued the study of light scattering, they observed what at first looked like fluorescence, but when this 'fluorescence' turned out to be polarized, its connection with light scattering became clear; that is, light scattering with modified frequencies: hence the Raman effect. C.V. Raman won the Nobel Prize in Physics for his work in 1930. Raman spectroscopy, since its onset, has been widely employed in many fields as an analytical tool for characterization and diagnostics [50, 51]. Raman measures the inelastic or symmetric vibrational stretching via light scattering detection. In 1974 a phenomena involved with the Raman effect was discovered called SERS. Surfaced Enhanced Raman Scattering / Spectroscopy, or as it is more commonly known as, SERS was initially observed by Fleischmann and coworkers while studying Raman scattering signals from pyridine (PYD) on roughened/colloid Ag surfaces [52]. At the time of its discovery, the investigators did not attribute the amplification of the spectra to anything in particular

and just coined it “Giant Raman”. Even today, as more research has been done on the SERS phenomena, the origin of the SERS effect is a subject of debate. However, there are two generally accepted mechanisms that contribute to the SERS effect on coinage metals like Au, Ag, and Cu, and they are the charge transfer (Ch-T) and electromagnetic (El-M) effect mechanisms [53]. Ch-T has a short range effect while El-M has a long range effect [54]. The El-M effect is thought to contribute the largest fraction to SERS signals. It is observed due to surface curvature/ nano-structure of the metal, their surface plasmon resonances in the visible region, the strong localized electric fields produced at “hot-spots” resulting from the incident light. The Ch-T effect or chemical effect arises from photo-driven process that transfers change and alters the signatures of various systems and is believe to contribute to a lesser degree. Classically, it was assumed that Au, Cu, and Ag were the only three metals compatible with SERS, due to their free electrons where the surface plasmon can be excited via near IR and visible light [55,56]. Other non-coinage metals were deemed inactive since their surface plasmon resonances would be difficult to excite, and only weak Raman spectra could be obtained via electrodeposition of the metal of interest onto a SERS substrate. However, in the late 1990s, with the introduction of confocal Raman instruments, basic transition metals Pt, Co, Ni, and Fe displayed surface Raman signals, and now many nanoparticles fabricated of these metals also induce the SERS effect [57,58]. Some advantages of employing SERS is the ability to study surface bonding and reactions that are relevant to catalysis and it significantly increases the relatively weak signals of the robust method of Raman scattering. In addition, the influence and application of SERS resides in its structural capability to identify chemical species and obtain mechanistic information in many fields

such as bio sensing, material science, and catalysis [59]. Thus, it is an ideal tool for electrochemical catalysis and experimental analysis.

1.6 Goals of research

We propose to investigate the reaction mechanism involved with the electroreduction of CO_2. By employing enhanced Raman spectroscopy on multifunctional SERS substrates that act as catalyst and amplification materials we hope to increase the possibility to detect the reaction species in progress. This is expected to advance the understanding of the CO_2 conversion process and contribute to the efficiency of Carbon Capture Storage and Harnessing (CCSH) technologies. Herein we discuss the synthesis and optimization of multiple dual catalysts and SERS substrates as well as preliminary in-situ detection experiments to elucidate the reaction mechanisms by the observation of key intermediates.

2 Experimental Methods

1. Nano- & patterned substrates

1.1 Preparation of Nano-triangle and Nano-metal bowls

For the preparation of nano-triangles and nano-metal bowls, we started with a clean substrate (e.g. graphite or glass) then spin coat and an optimized 1% solution of 1000nm polystyrene beads in (1/400) Triton-X/MeOH solvent. The substrate is then spun at 250 rpm to obtain a monolayer of beads, oven dried at 50-80°C for 1 minute. This was followed by electron beam evaporation or sputter coating of the metal (e.g. Au & Cu) on the monolayer of beads substrate, and finally tape, dichloromethane (DCM), and sonication lift-off to remove only the beads resulting in the nanostructure. (Adapted from [60], Fig 12A)

1.2 Preparation of Roughened Copper

Electrochemically cycled or roughened copper was prepared with a copper sheet cycled between 0 to 1 V at a 100 mV/s sweep rate in 5mM pyridine/10mM KCl solution against a reversible hydrogen electrode (RHE) RE, Copper WE vs. Pt (platinum) CE. In addition, cycling, 20 sweeps, between -2V and 1.2Vat 100mV/s sweep rate in 13mM KCl solution in 3 electrode cell with Pt CE, Copper WE vs. Pt pseudo reference.

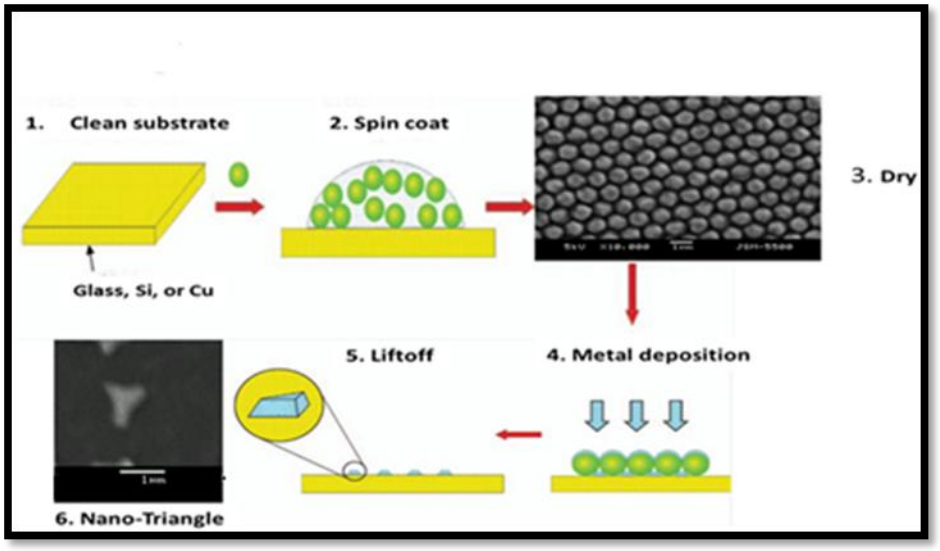

Figure 12A: Sample nano-triangle copper fabrication via nano-sphere lithography diagram [60]

2. Nano-porous substrates

2.1 Preparation of nanoporous copper (NpCu)

Two Al:Cu alloys of 30 at% Cu poured at 800 and 600 °C were employed to fabricate NpCu. Chemical and electrochemical etching of the Al was done in aqueous 6 M NaOH at 80 °C and a constant current of 50 mA/g for 24 hrs. Residual base was removed by submerging in DI H_2O for 24 hrs. Reduction of NpCu in H_2 atmosphere for 2hrs at 450 °C and subsequently at 100 °C overnight reduction results in oxide free porous copper (Fig 12B)

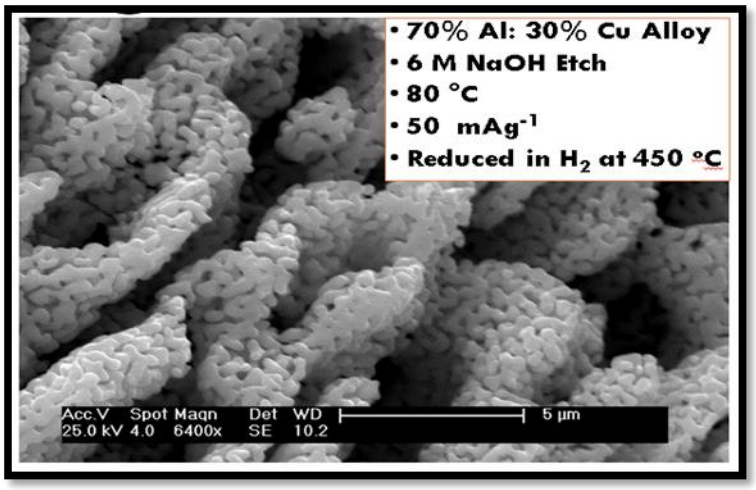

Figure 12B: Sample nano-porous copper fabrication conditions

2.2 Preparation of NpCu samples for SERS measurements

NpCu samples with various pore sizes were subjected to SERS experiments by first submerging the NpCu in 99.8% anhydrous pyridine (Sigma-Aldrich Co.) for 24 hrs. Then moving the NpCu to a petri-dish and submerging in DI H_2O, then remove non-adsorbed pyridine species and H_2O for SERS studies.

3 Instrumentation & Characterization

3.1 Renishaw Raman & Spectro-electrochemical flow cell

The Raman spectra were recorded via Renishaw Smiths Raman IR Microprobe using excitation line 632.8 nm He/Ne ion laser with 5X objective, 100% laser power of 7.2 mW. Electrochemical experiments were conducted on CHI604 Electrochemical Analyzer. In-situ spectro-electrochemical flow cell utilized a Copper WE, and Pt CE against a Pt-pseudo RE. All experiments were conducted in aqueous 0.1M $KHCO_3$ in 0.01 M KCl (Fig 13).

3.2 Scanning Electron Microscope (SEM)

An XL-30 Environmental-SEM with a secondary electron (SE) detector, an Energy Dispersive Spectrometer (EDS) and an internal TV camera (CCD) for imaging at 1.2E-4 torr were used.

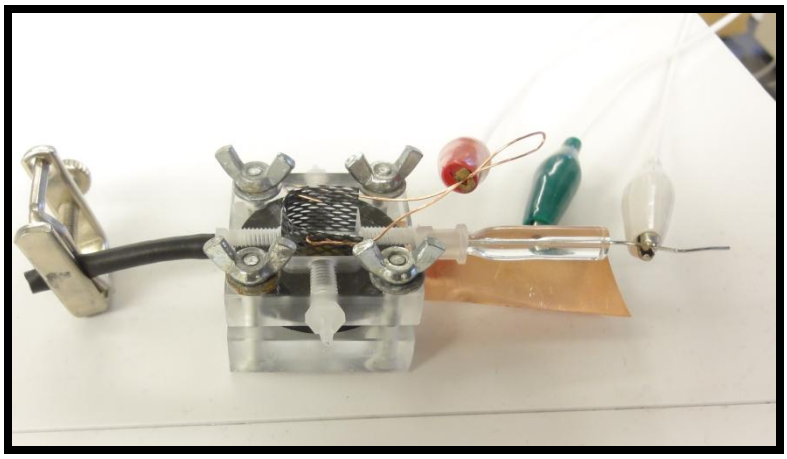

Figure 13: Spectro-electrochemical flow cell. Red clip Pt CE, Green clip WE, and White clip Pt-pseudo RE. Flow solution in and out through the front and back nozzles.

3 Materials

The synthesis of nano-triangles and nano-bowls afforded various substrate morphologies depending on substrate type, lithography mold, metal deposition, and liftoff technique employed. For instance, a clean graphite sheet substrate, with 200nm to 500nm polystyrene beads patterned in a monolayer, with subsequent gold (Au) sputter coating and sonication liftoff created Au nano-bowls (Fig 14 A&B). The nano-bowls features had diameters ranging from 100nm to 500nm and ligament or presumptive triangles size ranging from 50 -200nm. These sizes correspond to the beads sizes. Due to the non-uniformity of the beads size in the monolayer, which exists partially out of phase due to packing defects, the nano-bowls fail to share common sizes.

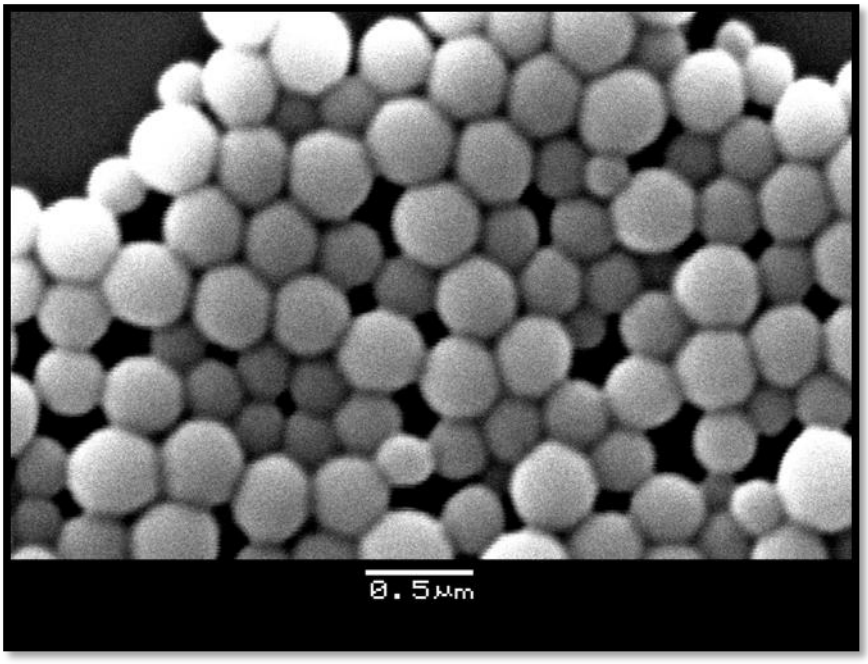

Figure 14A: SEM image of 'partial' monolayer or multilayer of (200nm-500nm) polystyrene beads before metal deposition and liftoff.

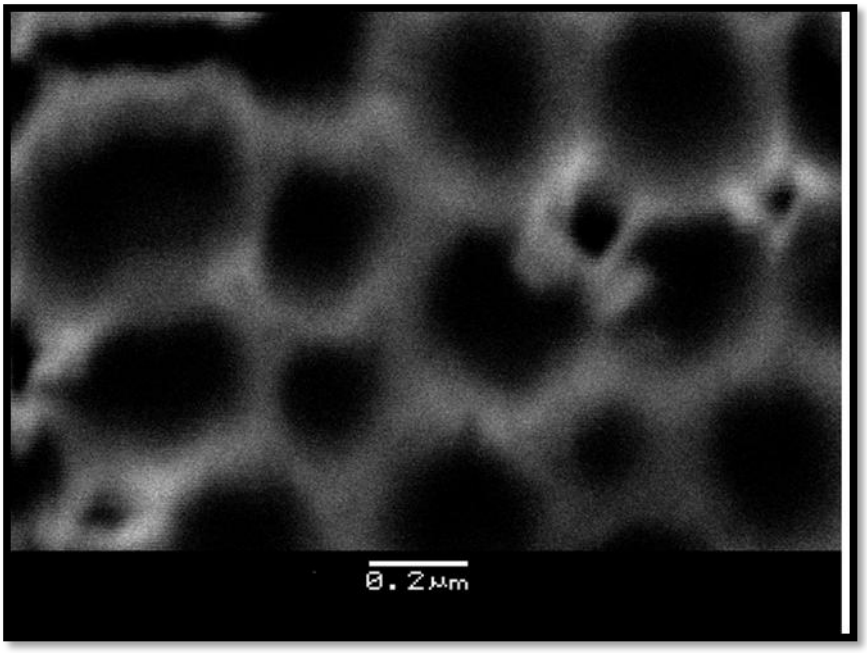

Figure 14B: Nano-bowls of gold SEM image

Also, "expanded" nano-peaks were fabricated via a similar process that involved silicon wafers as the clean substrate, followed with 1000nm monolayer beads deposition (Fig 15A). Using bigger, 1000nm beads, led to avoiding non-uniformity of the metal mold and fabricate a SERS active substrate. Then, subsequent gold or copper electron beam evaporation with sonication, dichloromethane (DCM), or tape liftoff is performed. The silicon substrate gave "expanded" nano-peaks and nano-squares morphologies after either sonication or tape liftoff with DCM liftoff being ineffective (Fig 15B).

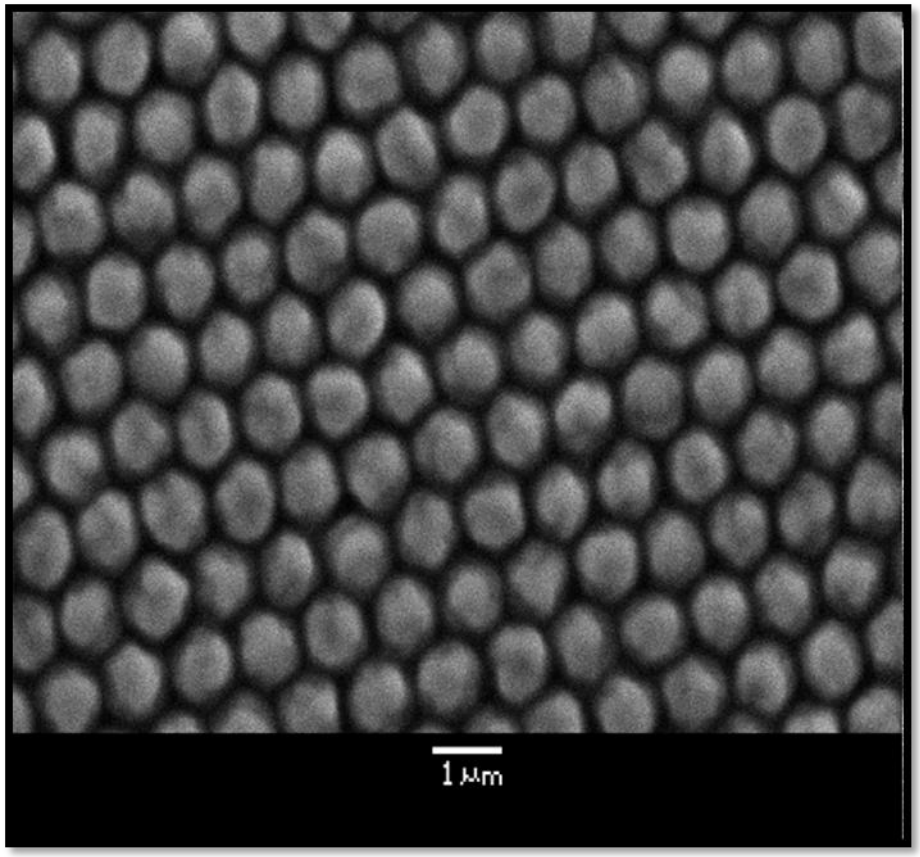

Figure 15A: SEM image of monolayer of 1000nm (1um) polystyrene beads before metal deposition and liftoff.

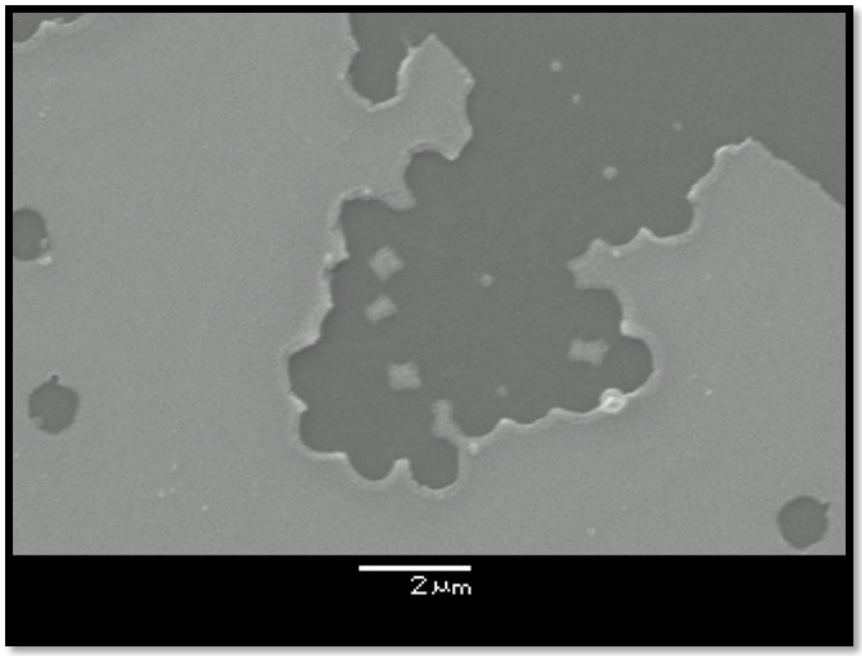

Figure 15B: Gold "expanded" nano-peaks and nano-squares on silicon SEM image

Finally, nano-triangles in a honeycomb shape were made with graphite and copper sheets as substrates; followed with ~1000nm monolayer beads deposition, gold or copper electron beam evaporation, then tape liftoff. Both substrates gave nano-triangle morphologies that range in size of 1000nm in length and 200nm ligament size (Fig 16 top). The tape lift off is the best method for removing the mold/ beads but almost always results in a partial remove as shown in Fig 16 (bottom). While sonication is also an acceptable removal method for our system, it cannot be utilized for long periods of time since the heat generated will remove the polystyrene beads ands and the deposited metal. DCM simply removes both constructs in a sheet and is an unacceptable method of liftoff for our fabrication system. The morphologies of the triangles appear less defined to the electron beam evaporation. Physical vapor deposition (PVD) would most likely result in more defined nano-triangles with our current lithography methods. Also employing PYD could also induce greater SERS.

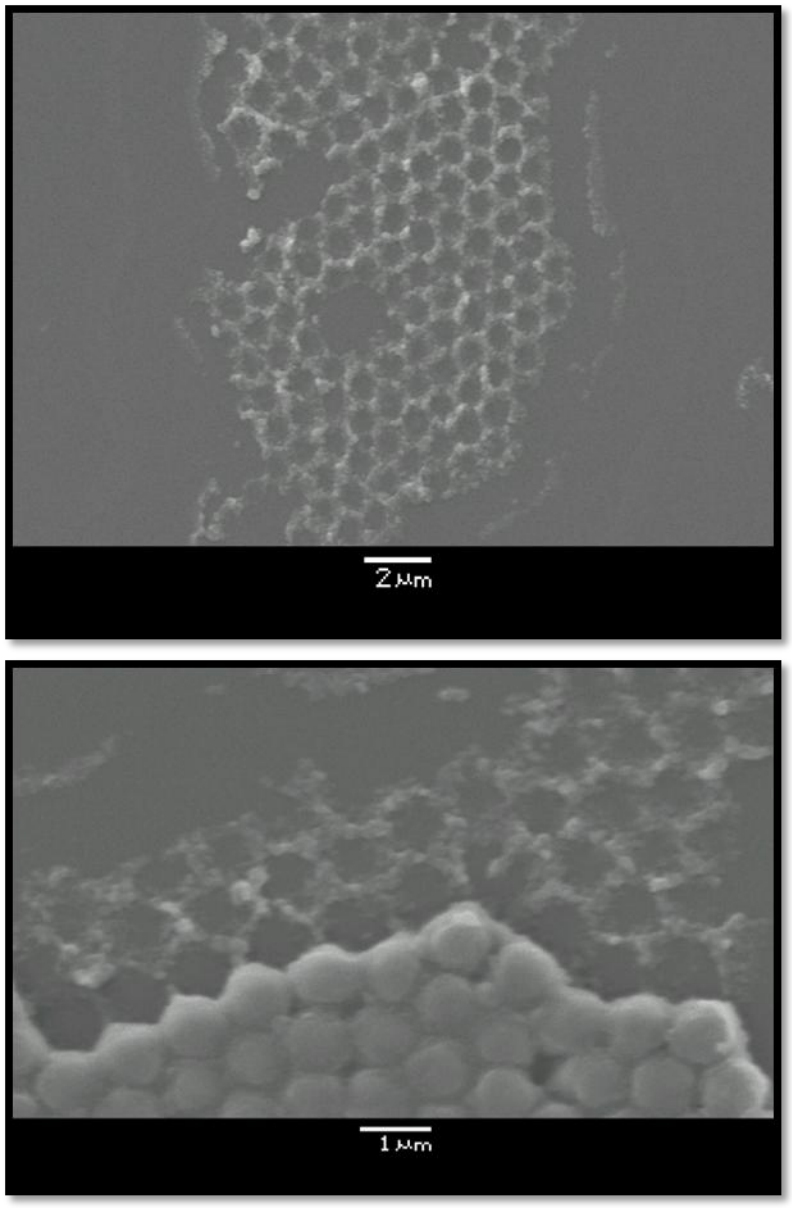

Figure 16: Copper nano-triangle on graphite SEM image. Complete removal of polystyrene beads and nano-triangle structures (Top). Partial removal of polystyrene beads and closer look at nano-triangle morphologies (Bottom).

Electrochemically cycled/ roughened copper sheets were also made in our lab, as they have been noted to induce SERS and would be adequate standards for the SERS substrate experiments conducted. Two methods were used for the roughened copper SERS substrates synthesis. One was done very closely to the literature involving a copper sheet

cycled via cyclic voltammetry (CV) in 5mM pyridine (PYD) and 10mM KCl solution to chemisorb pyridine during the roughened process (Fig 17 A&B) [61]. The second involved roughening with ~10mM KCl then adsorbing pyridine after roughening for comparison purposes (Fig 18 A & B). Both substrates show rough characteristics for SERS, however the current required for a CV seems to be much larger when employed in KCl electrolyte with a larger Pt CE than in pyridine/KCl solution with a smaller Pt CE.

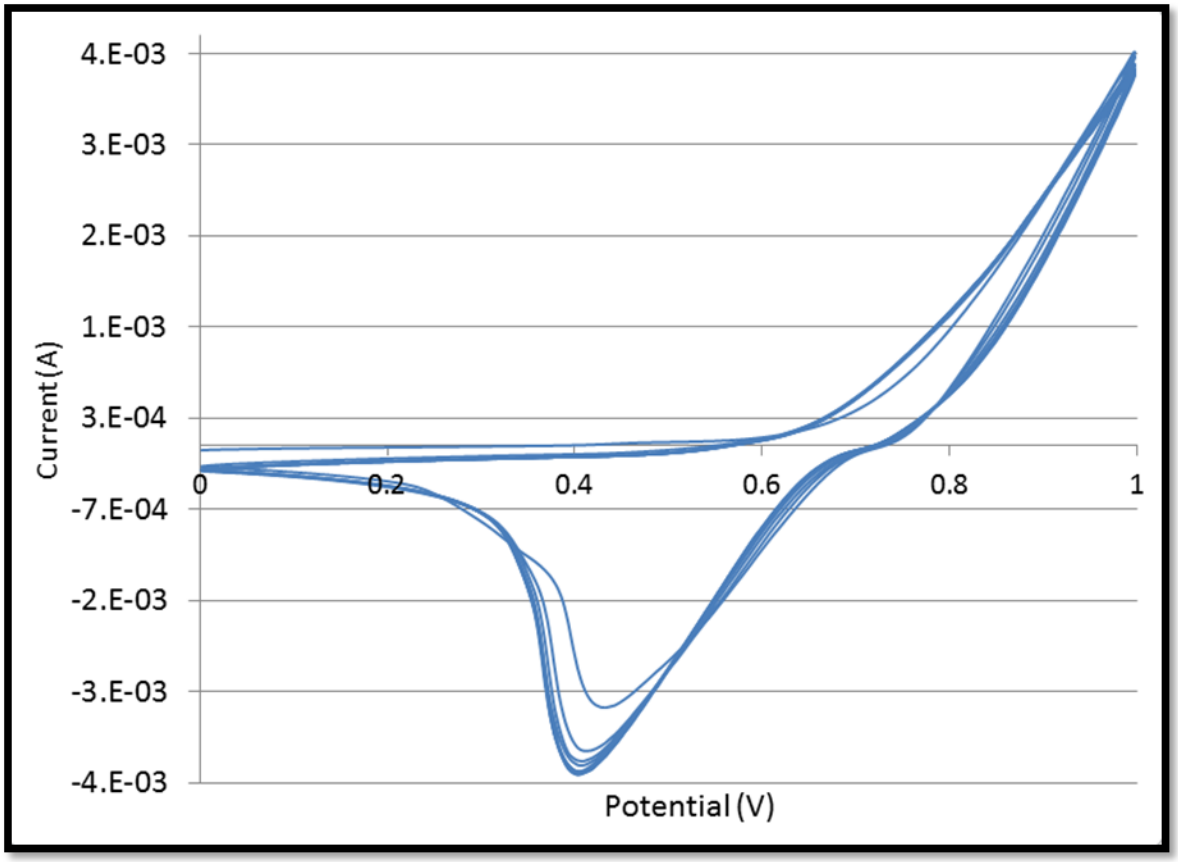

Figure 17A: CV of copper sheet in 5mM pyridine and 10mM KCl sweep 0V to -1V vs. RHE.

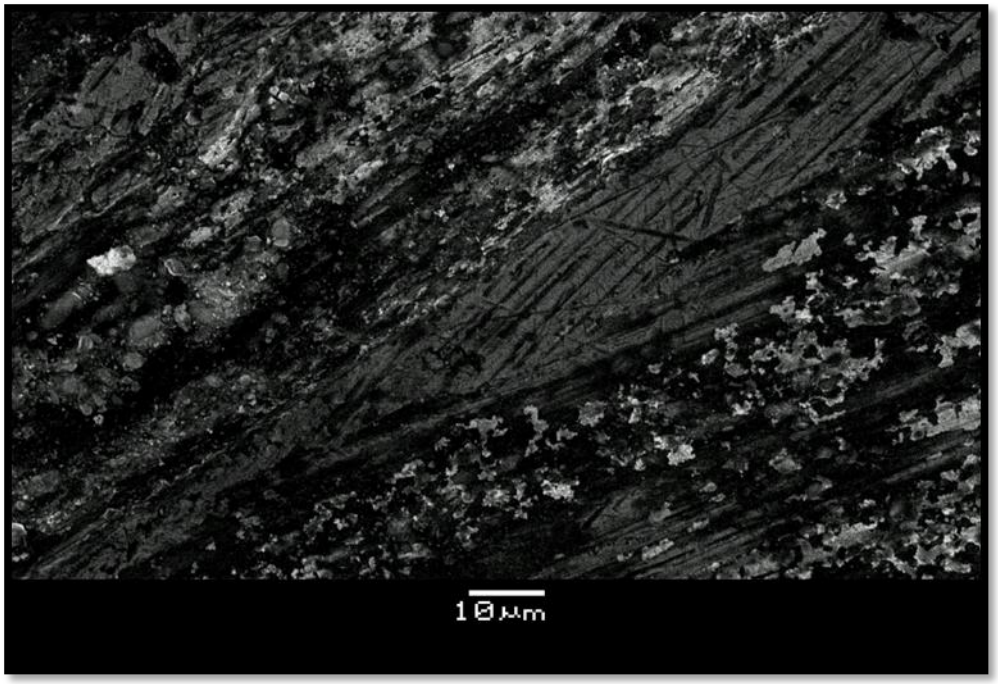

Figure 17B: SEM image of CV roughened copper sheet in 5mM pyridine and 10mM KCl

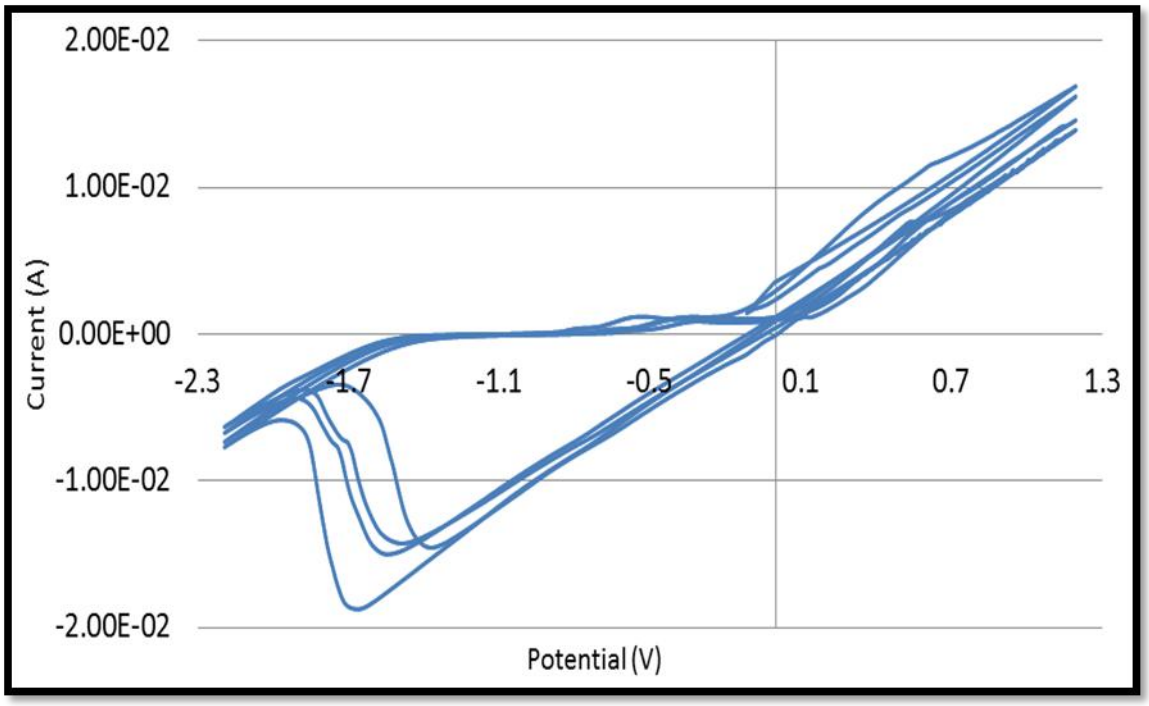

Figure 18A: CV of copper sheet in 10mM KCl sweep 1.2V to -2V vs. Pt-pseudo RE

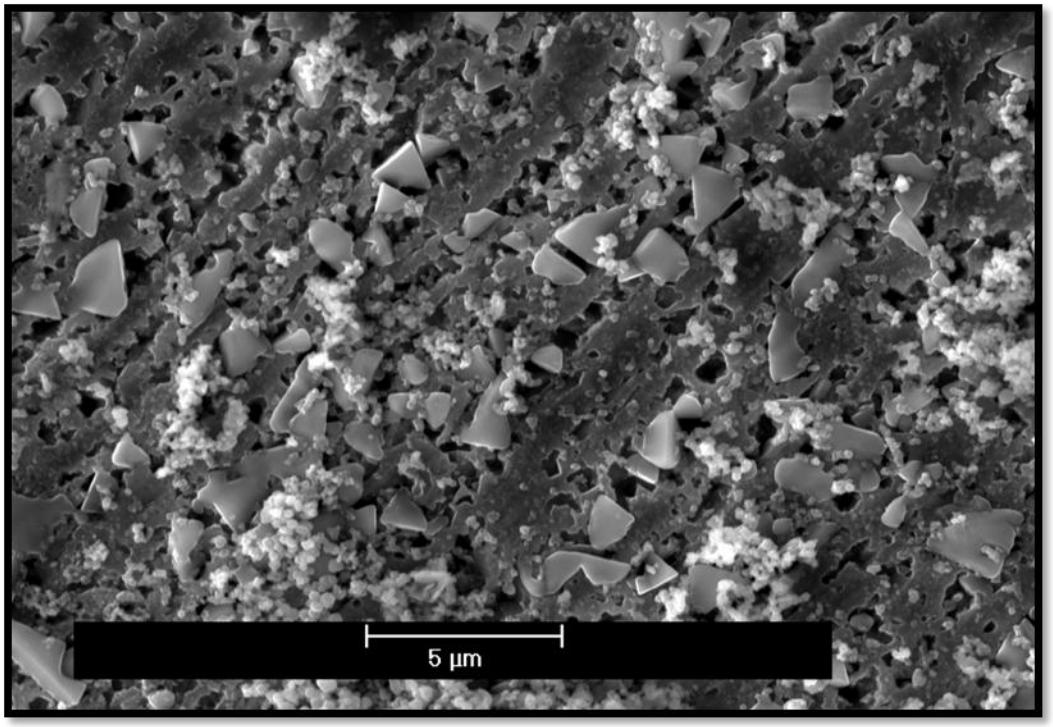

Figure 18B: SEM image of CV roughened copper sheet in 10mM KCl

Nano-porous copper was fabricated via a number of methods to generate pores (vacancies in the structure) ranging from 25 nanometers (nm) to 2.5 microns (um) in size and ligaments (solid structure surrounding vacancies) ranging from 50 nm to 1.2 um (Fig 19). To achieve this two alloys were used. Then, with these alloys, we removed the Al via etching in a strong base sodium hydroxide (NaOH) at temperatures 25 ℃, 50 ℃, 80 ℃, and 120 °C. Using 1M NaOH we can generate NpCu partial etch with some alumina (Al_2O_3) and 6M we obtain mainly NpCu with some oxide. The 6M etched NpCu structure has characteristic "pore within pores" structure, for measurments the smallest pores were noted (Fig 20). In addition, we utilized electrochemical methods such as applying a current from 5 mA/g to 1 A/g to aid in the etching process and further increase the variety of porous structures fabricated. Due to the oxide present after NaOH removal, high temperature reduction under hydrogen (H_2) atmosphere removes most of the oxide

(Table 1). Also, upon reduction, the morphologies of the NpCu change, generally resulting in an increased pore size but pores can also be unchanged, decreased in size or have the appearance of a rougher or smoother effect on the morphologies (Fig 21). Using Brunauer-Emmett-Teller (BET) it was found that the average surface area of our NpCu was 10 m^2 g^{-1}. In short, there are many properties that are characteristic of each individual NpCu fabricated and these variations can be exploited for SERS and catalysis.

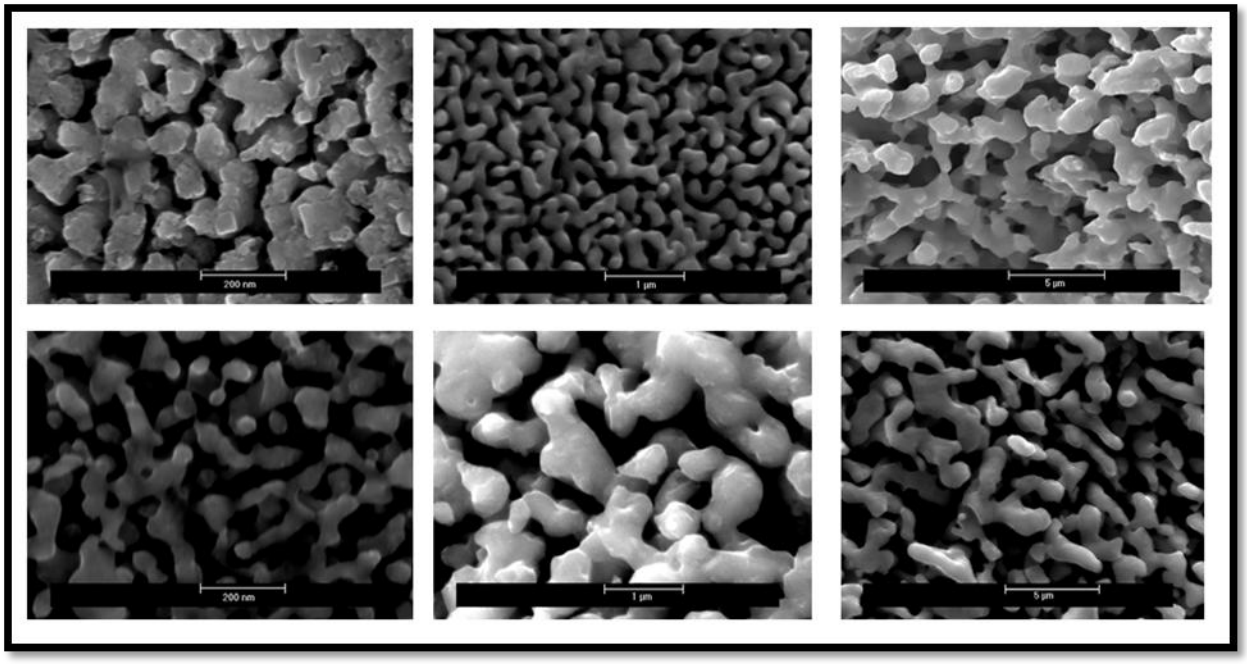

Figure 19: Distribution of NpCu pore sizes made, increasing from right to left and the top down. Each column: right, center, and left have similar SEM standard length bars for comparison. Smallest pores, top right around 25 nm with an average pore size of 35nm. Largest pores, bottom left are around 2.5microns (2500 nm) with an average pore size of about 1.5 microns.

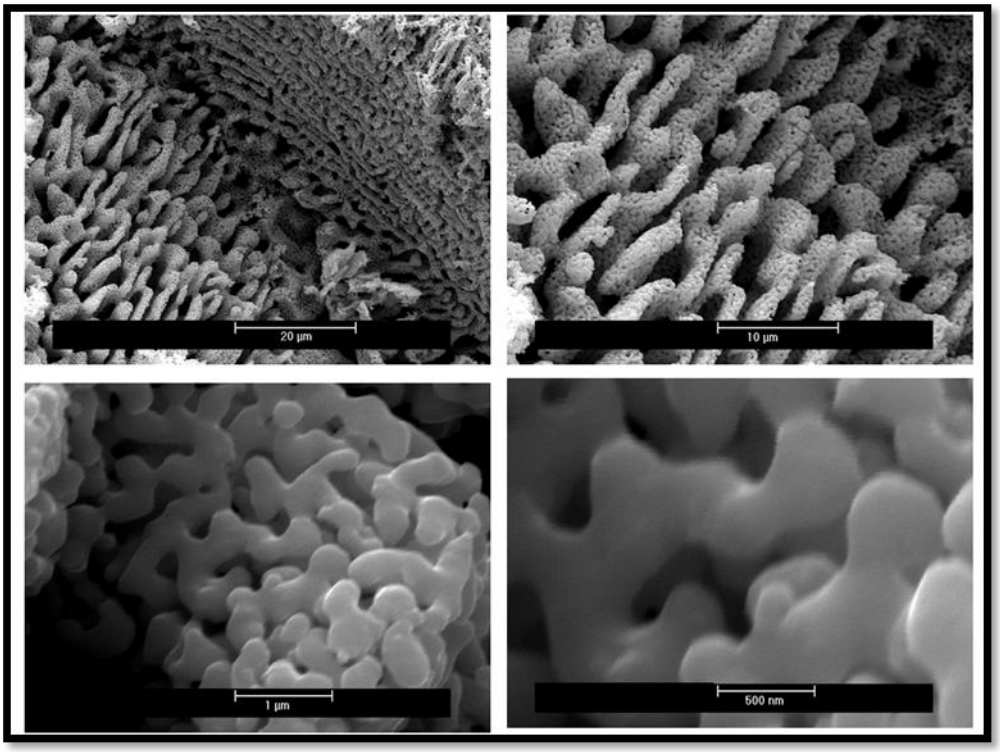

Figure 20: SEM image of NpCu "pore within pores" structure, zooming in on the same spot from larger pore structure to smaller.

Alloy Composition Before and After Reduction						
	Al:Cu alloy standard		NpCu Not reduced		NpCu reduced	
Element	Wt %	At%	Wt %	At%	Wt %	At%
Carbon	0	0	2.0	6.4	5.1	20.3
Oxygen	0.9	1.8	18.2	43.2	2.7	7.9
Aluminum	72.8	85.2	3.3	4.6	2.1	3.7
Cu	26.2	13.0	76.5	45.8	90.1	68.1
Total	100	100	100	100	100	100

Table 1: Display of EDS data of NpCu with an without reduction revealing higher levels of oxide on non-reduced NpCu. Carbon contamination in EDS analysis most likely due to NpCu on carbon tape during analysis.

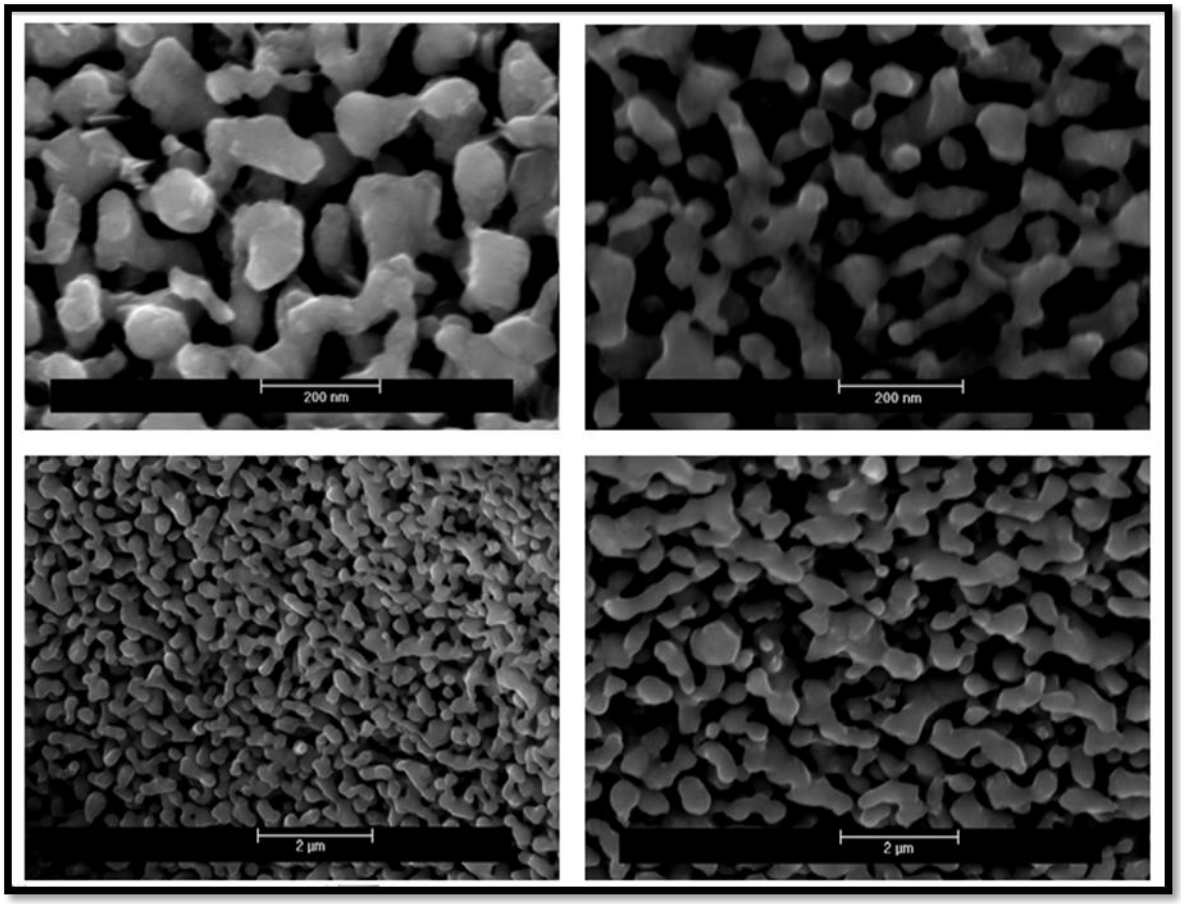

Figure 21: Effect of reduction shown. NpCu on the left have not been reduced while the same NpCu on the right has been reduced and a general increase in pore size can be seen.

4 Copper substrates SERS and Optimization

For each of these materials Raman spectroscopy was employed to test respective SERS enhancement capabilities (Fig 22). Only honeycomb nanotriangles (Nano-T), NpCu, and roughened copper (R-Cu) substrates (displayed in Figure 16, 12B, and 17B) were tested but Nano-bowls have yet to be tested for SERS. When observing spectra of pyridine adsorbed on copper substrate, there is a noticeably stronger group of vibrational bands aroung 1000 cm^{-1} in each Raman spectrum. As a result, the bands that are centered around 1000 cm^{-1} will be the main focus for SERS throughout the length of this discussion. These peaks correspond to the breathing modes of pyridine in bulk solution and adsorbed onto a metal, in this case copper. The vibration bands are described as "breathing" due to the combination of the pyridine resonance structure's simultaneous symmetric stretching inward with C-C and C-N variations found via computation [62]. It is possible to think of pyridine adsorbed onto copper as a "super-molecule" of Cu-N, in which the excitation of plasmon electrons gives rise to a geometry or vibrational change of the bound pyridine and thus results in shifts in the specific signatures of the pyridine Raman scattering. SERS resonance effects due to transitions within the specific metal that gives rise to excited state displacement of a bound adsorbate are thought to be the cause of the modal frequency shifts. The excited state geometry changes of the bound pyridine can also give rise to resonance enhancement, as with all Raman scattering. However, there must be a chemical to surface bond such that charge displacement interactions in the excited state still have relatively normal modes in the excited state being detected. The normal breathing modes of pyridine around 1000 cm^{-1} are V_1 (980 cm^{-1}), V_{12} (1010 cm^{-1}) and V_{18a} (1030 cm^{-1}) with modes V_1 and V_{18a} being the strongest

and second strangest vibrational bands, respectively. When measuring the SERS activity for each substrate, the materials display good enhancement that is comparable to a pyridine solution standard spectrum with notable shift in frequency of each individual substrate (Fig 23). A noteworthy observation is that the different substrates shift the vibrational modes to different wave frequencies. This is thought to be due to the distinct substrate environments and nanostructure specific plasmons, where the pyridine adsorption occurs that contribute to the El-M and Ch-T effects to a different extent, however this is mainly conjecture based on these observations [63].

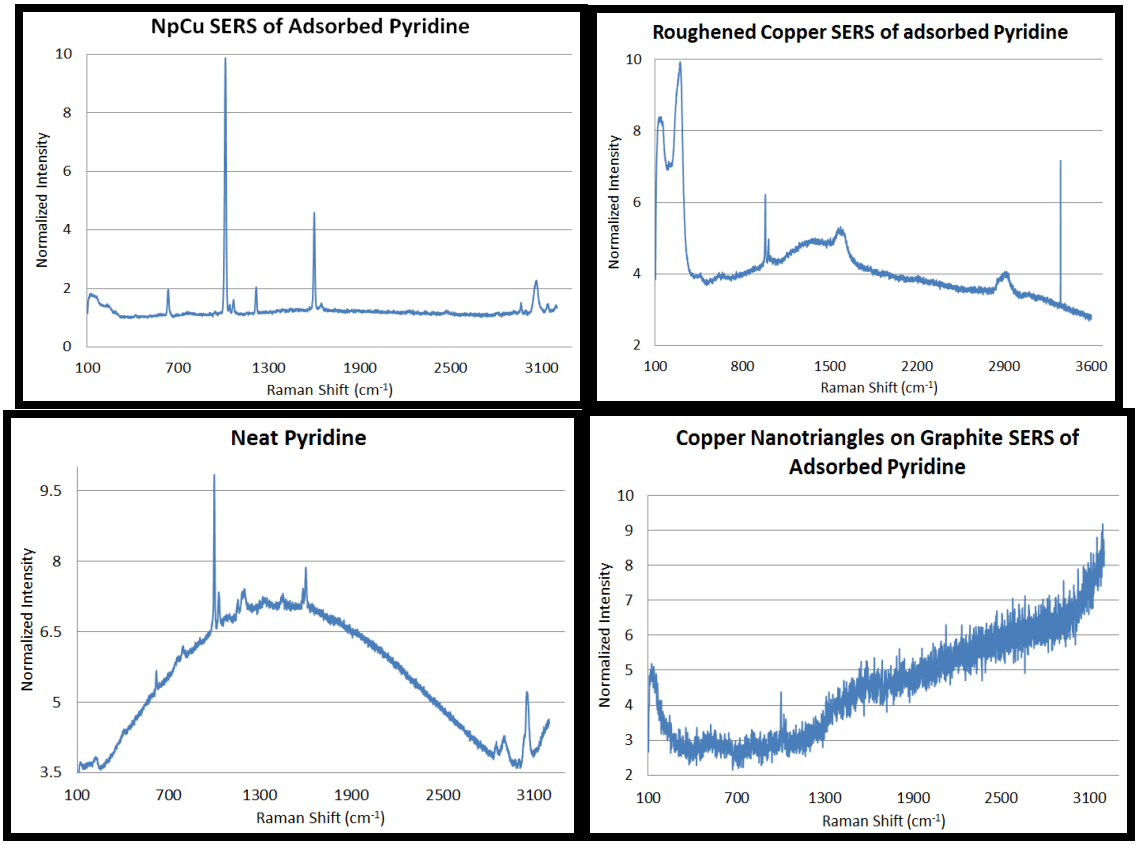

Figure 22: The different spectral signature of bulk pyridine and SERS materials. The vibrational modes, V_1,V_{12},and V_{18a}, of pyridine breathing shifts in cm^{-1}: Neat PYD 989.84, 1003.73,1035.23; NpCu 1020.58,1064.56; R-Cu 982.35, 1008.07; and Nano-T 1019.7, 1037.02.

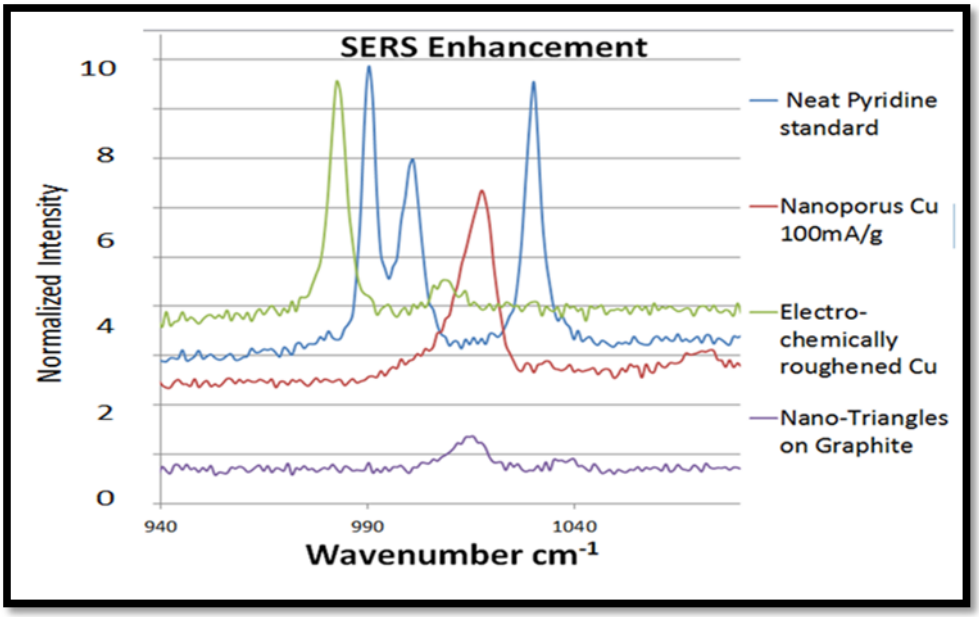

Figure 23: SERS substrates in comparison to bulk pyridine, shows promising enhancement for Cu SESR applications

Considering the substrates NpCu and Nano-T which were fabricated in this system, NpCu appears to induce greater enhancement than Nano-Ts observed in the spectra. So for electroreduction of CO_2 on copper it seems prudent to use NpCu because of its enhanced spectral signal observed its potentially large catalytically active surface area. As a result, the flexible fabrication parameters for generating the NpCu material was exploited by altering the etching methods to obtain the various pore sizes and the optimum SERS effect. Understanding the morphological characteristics correlated with SERS can be beneficial to utilizing a multifunctional amplification catalyst for intermediate detection. The multifunctional substrates are catalytically active since they are composed of copper and also can enhance spectra to different degrees based on the pore and ligament sizes of the substrate. We experimented with many pore sizes and their corresponding Raman spectra after submerging NpCu in neat pyridine for 24hrs and

found the optimum pore size for NpCu (Fig 24A & B). Our results were that the optimum SERS pore size was around 500 nm and larger ligament sizes around 500 to 1000 nm induce the greatest SERS effect when a 633 nm laser is employed for measurements. Other researchers have investigated NpCu SERS revealing a similar trend however, their results are limited to pores under 200nm [64]. Our investigation provides a more complete analysis of NpCu SERS, by extending the range pore sizes tested displayed in figure 19. Furthermore, there is an oxide layer formed on the NpCu catalyst when left in normal atmosphere. We examine the conditions for the removal of the oxide layer from the copper catalyst as a function of H_2 concentration and temperature (Fig 25A). An increase in pore size after reduction is displayed in figure 21. Generally there is also a distinct increase in SERS amplification, normally 2-10 fold, when reduction is utilized on NpCu. Also, when NpCu was reduced for extended periods of time, a greater SERS effect was observed (Fig 25B).

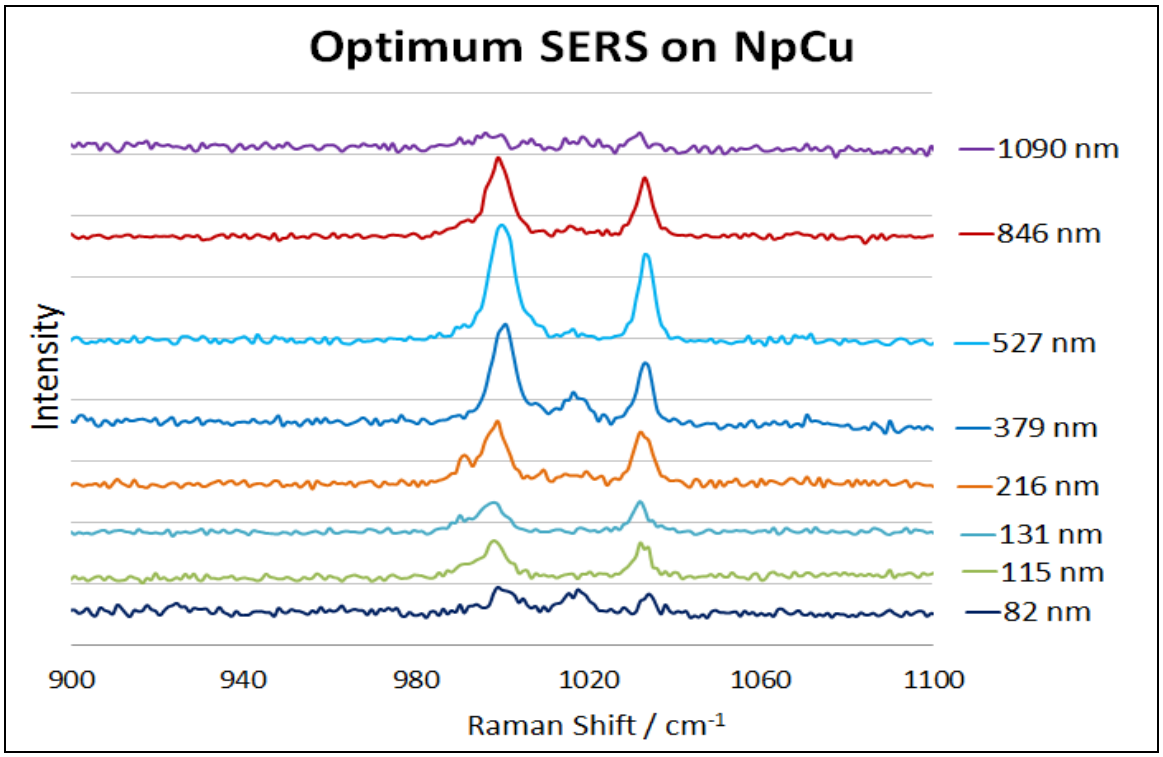

Figure 24A: NpCu SERS at various pore sizes using pyridine.

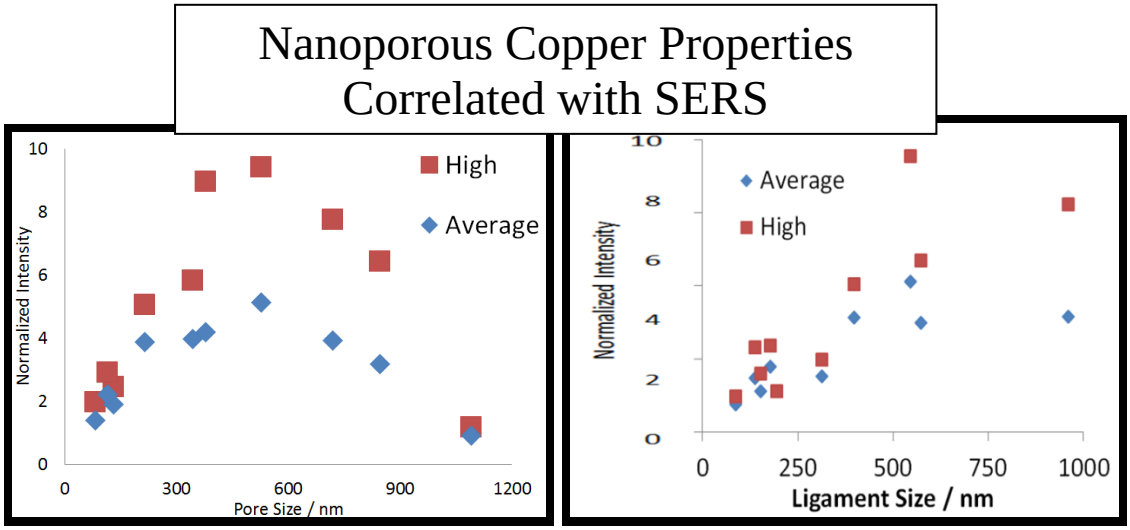

Figure 24B: NpCu characteristics of pore size and ligament size and their relationship with SERS pyridine enhancement. Reveals the optimum pore size for NpCu is ~500 nm. Also the ligament size show a more linear relationship that as we increase the ligament size the SERS amplification increase almost proportionally then plateaus at large ligaments.

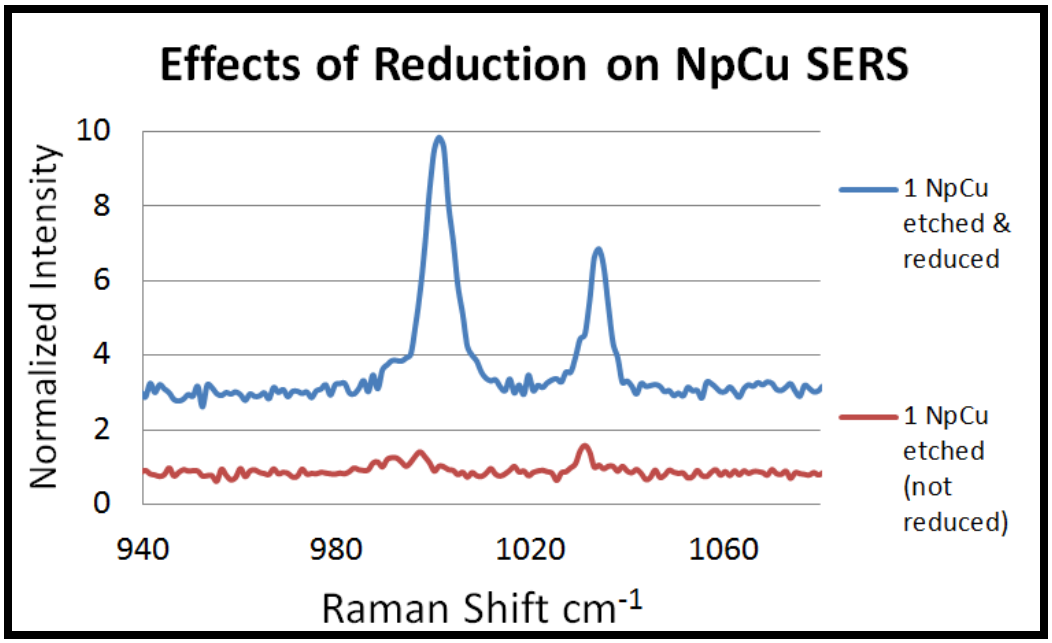

Figure 25A: The effects of reduction on SERS, essentially removing the oxide layer from NpCu and possible annealing the surface to increase the SERS effect of reduce NpCu enhancement over non reduced NpCu enhancement.

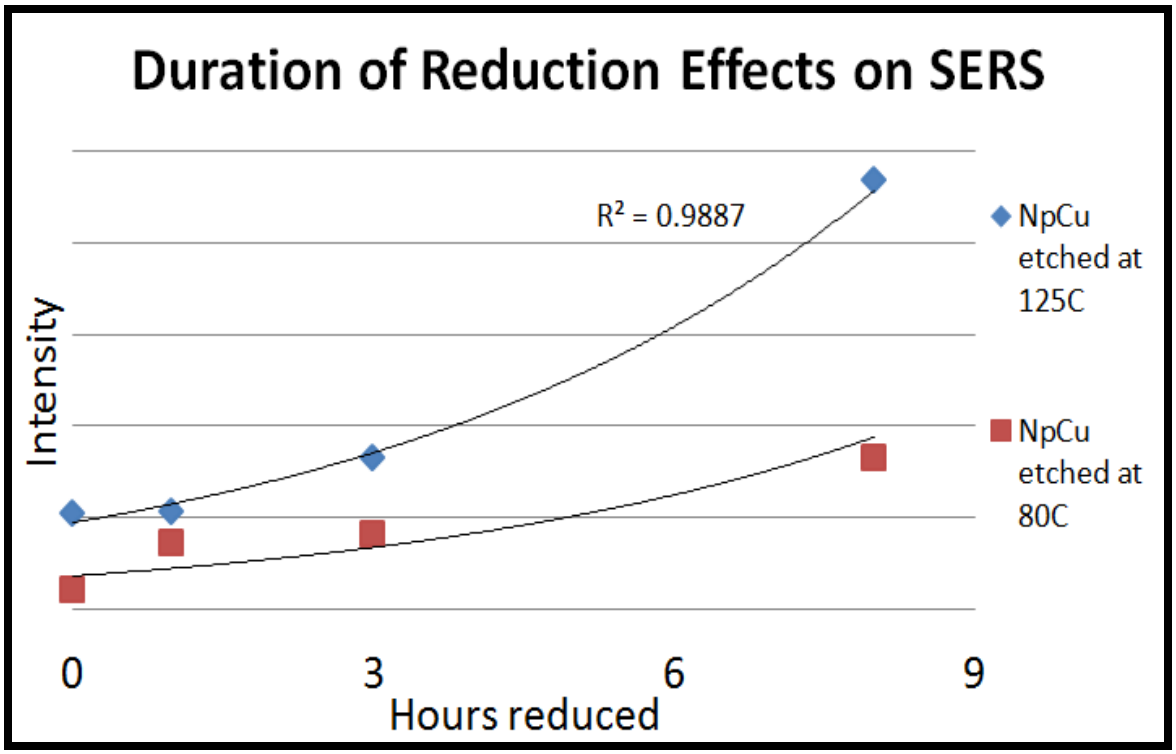

Figure 25B: A strong exponential relationship between increasing the duration of NpCu reduction and the intensity of SERS observed in spectra.

So far, the NpCu spectra and data shown have only been collected after neat pyridine adsorption on completely etched alloys. However, when adsorbing pyridine with KCl in solution or alumina on NpCu, greater enhancement is induced (Fig 26). In the addition to the difference in the peak intensity the vibrational modes of adsorbed pyridine are shifted compared to neat pyridine NpCu spectrum. The KCl in solution most likely roughens the surface and contributes, along with the porous structure, to the SERS via a combinatorial or cooperative mechanism. But the alumina contribution is still an enigma worth investigation, though it is probably due to an increased contribution of the El-M and chemical Ch-T effects in NpCu SERS.

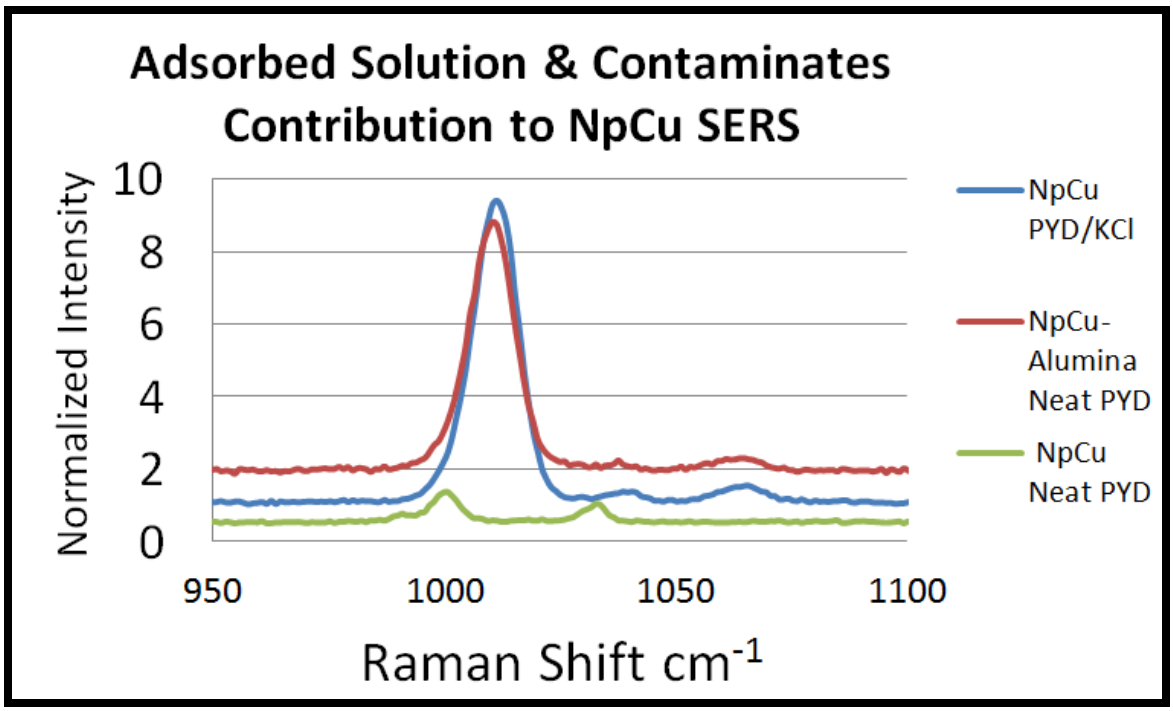

Figure 26: Display of the chemical effect on the structure and thus SERS of NpCu. A district increase in SERS via the introduction of chemicals like 5mM Pyridine (PYD)/10mM KCl soaking roughing the porous structure and alumina due to incomplete etching.

For the bulk our experiments, a 633 nm laser was utilized, but we also examined if there were other lasers that could be utilized that would add to the flexibility of the system

employing NpCu for CO_2 reduction intermediate detection. Thus, we ran UV-Vis on our NpCu and also tested our NpCu samples with a 514 nm laser (Fig27). The result was that the 514 nm induced greater enhancement and this was supported by the UV-Vis data. In addition to finding out the range of possible laser wavelengths that can be used for NpCu SERS, we aimed to identify what the SERS enhancement factor for NpCu was and how much of our sample was actively participating in SERS the amplification (Fig 28). Using the appropriate information we determined that our SERS substrate had an enhancement of 10^2 via this equation: G=[I(surface)/N(surface)]/[I(bulk)/N(bulk)], where G is the surface enhancement factor, I is the integrated intensity and N is the number of Raman active molecules [57].

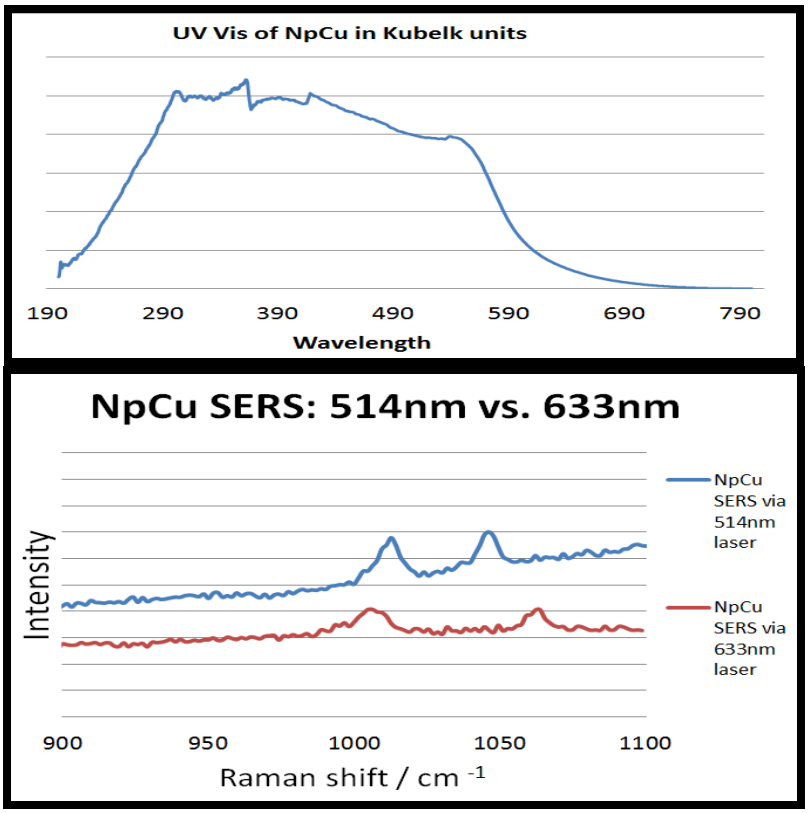

Figure 27: UV-Vis spectrum of NpCu showing a range of 190nm to 700nm wavelength laser could possibly be used for NpCu SERS. Different lasers 514nm and 633nm use for NpCu SERS reveal the 514nm induced greater enhancement and correlates with UV-Vis larger area.

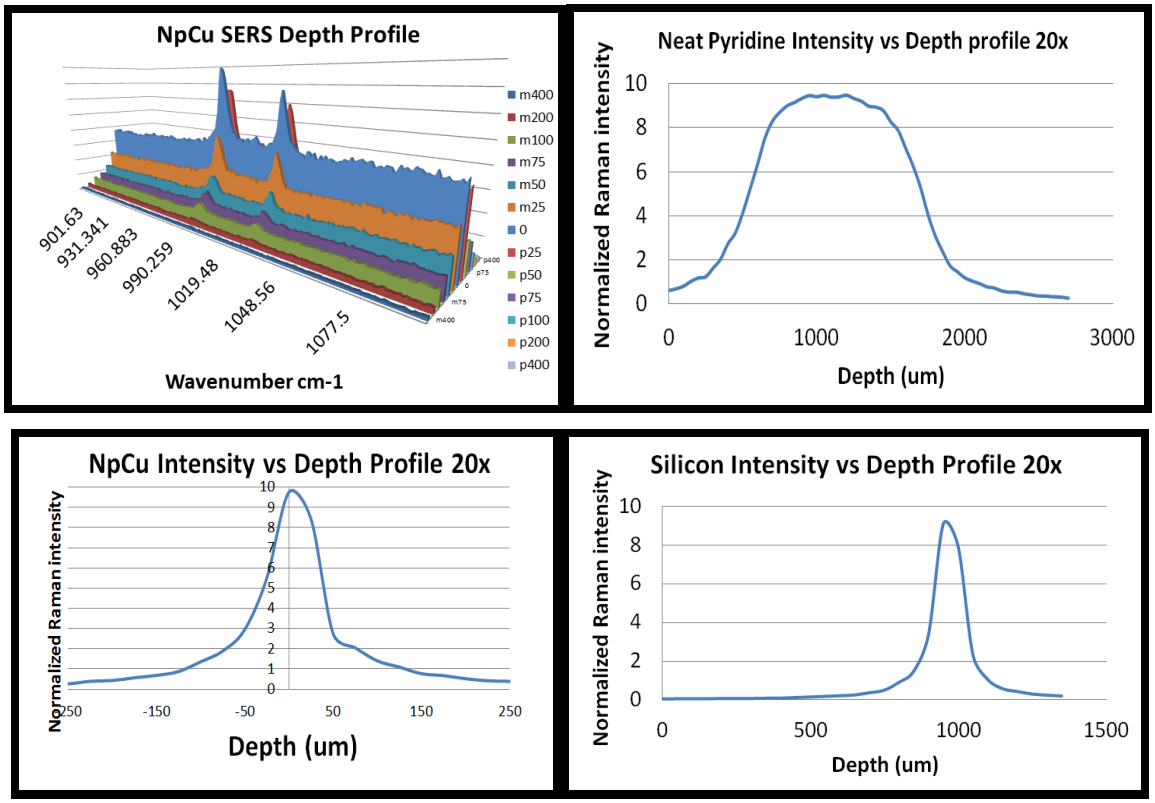

Figure 28: Depth intensity profile via 20X objective of Pyridine standard (top right) and NpCu (Top left) and Silicon standard (Bottom right) Also spectra of Npcu Intensity as a function of depth. The active fraction of material by depth of NpCu is around 200 microns, for pyridine bulk solution its around 2000 microns for a volume of 60 $mm^3$and 400 microns for silicon.

5 In-situ Electrochemistry and Raman

Following our experiments testing many of the characteristics of NpCu with our probe pyridine we proceeded to test its application for CO_2 reduction detection in-situ via a spectroelectrochemical flow cell displayed in figure 13. Also for comparison we also explored R-Cu's capacity for intermediate detection via Raman spectroscopy. For the three electrode spectroelectrochemical flow cell set up copper was employed as the catalyst/working electrode vs. a pseudo Pt (platinum) reference. Electrochemically filtered 0.1M bicarbonate ($KHCO_3$) and .01M KCl in deionized water saturated with bubbled CO_2 was flowed through the cell. Vibrational bands of 150, 1350, and 1600 cm^{-1} were observed for NpCu and R-Cu in this solution, these peaks were used as references when obtaining experimental controls. For NpCu when applying a potential of -1V vs. a Pt pseudo reference SERS spectra of CO_2 reduction on NpCu exhibits vibrational bands around 1010, 1065, 1350, 1600 and 2050 cm^{-1} (Fig 29). When applying a potential of -1.5V multiple vibrational bands are present: around 545, 630, 780, 1010, 1065, 1210, 1350, 1410, 1600, 1700, 2040, 2600, 2830, 2880 cm^{-1} (Fig 30). Applying a potential of -2V vibrational bands present are around 550, 710, 1065, 1350, 1600 cm^{-1} (Fig 31). For -2V and sometimes for -1.5V potential holds different spectra have been observed due to the high activity of potential water splitting into H_2 and gaseous hydrocarbons that disrupt the laser focus and electrode connection to the copper surface for optimum SERS and detection. Thus collecting some spectra is a bit of an obstacle for high range potential holds.

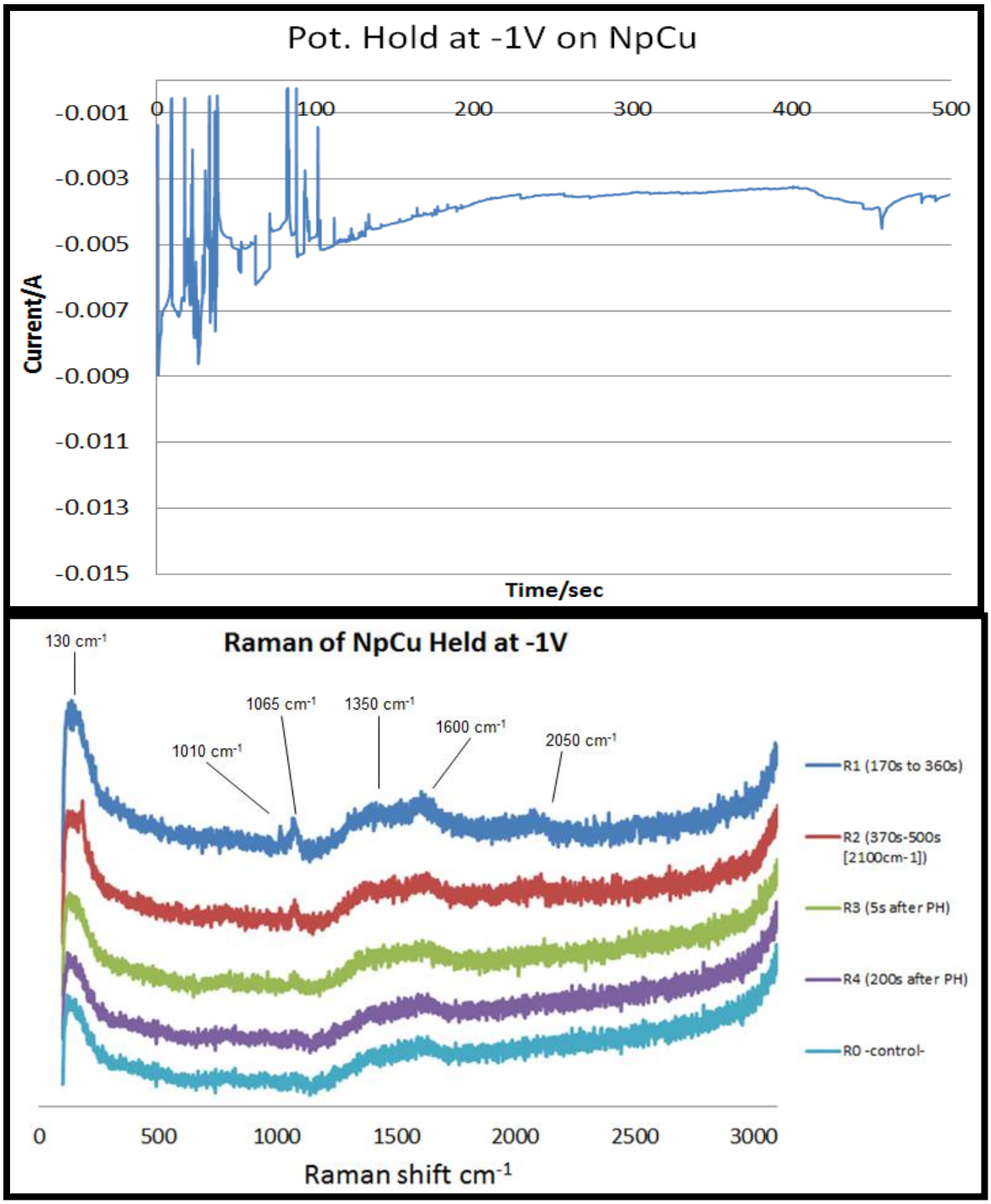

Figure 29: NpCu potential hold (PH) at -1V for 500s (top) and Raman of NpCu CO_2 reduction during and after the PH (Bottom) also with R0 Raman control of NpCu and CO_2 saturated solution with no potential applied.

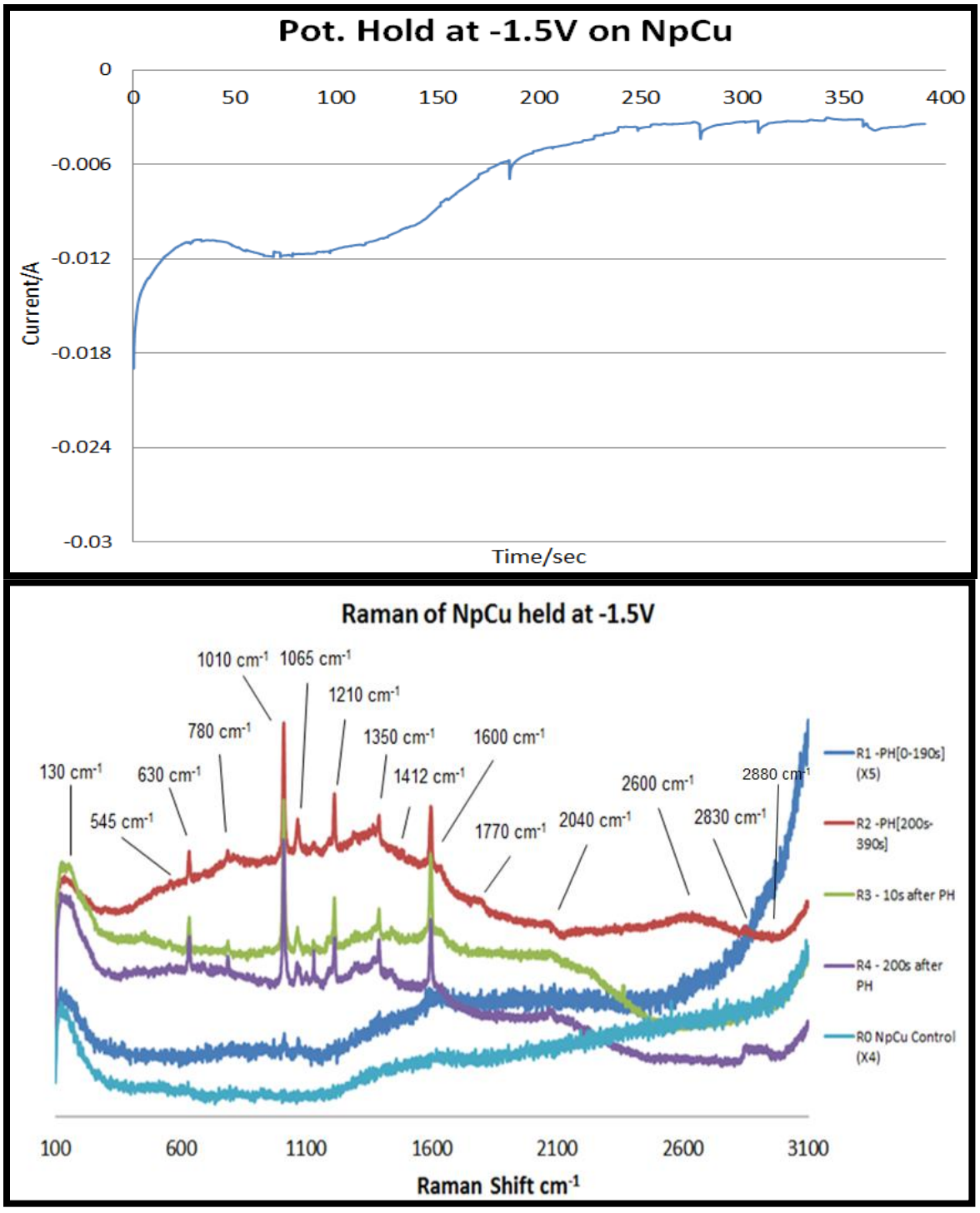

Figure 30: NpCu potential hold (PH) at -1.5V for 390s (top) and Raman of NpCu CO_2 reduction during and after the PH (Bottom) also with R0 Raman control of NpCu and CO_2 saturated solution with no potential applied. Note R0 and R1 are multiple by 4X and 5X for comparison purposes.

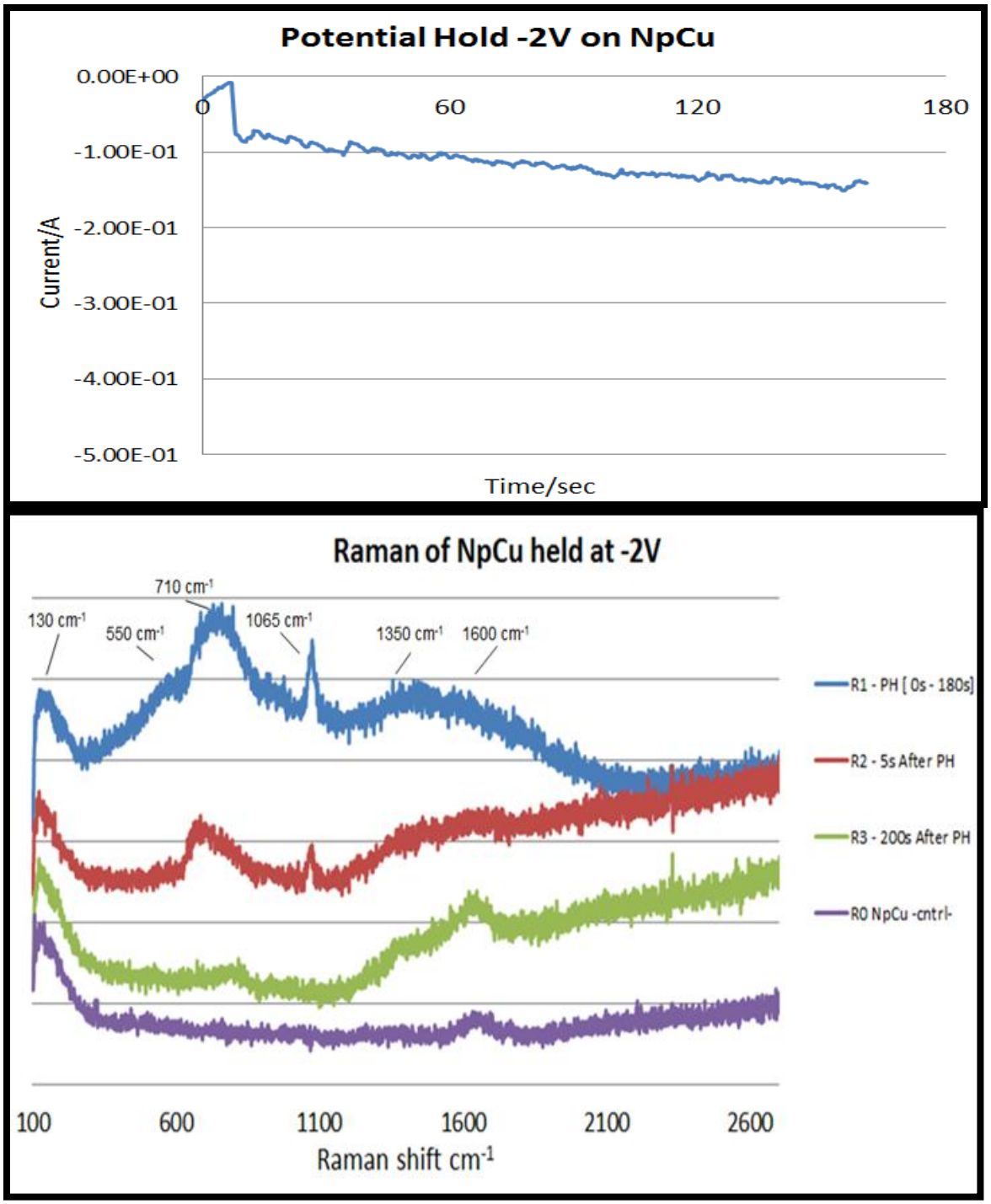

Figure 31 : NpCu potential hold (PH) at -2V for 180s (top) and Raman of NpCu CO_2 reduction during and after the PH (Bottom) also with R0 Raman control of NpCu and CO_2 saturated solution with no potential applied.

For R-Cu when a potential of -1V or 1.5V is applied a similar bands at 250, 780*, 1065, 1350, 1600, 2040, 2450-2700, 2880 cm^{-1} are observed. These bands are thought to be similar species to the observed for NpCu (Fig 32 & 33). The reoccurring presence of these vibrational band on both R-Cu and NpCu may indicate that it is the surface species or intermediate of CO_2 reduction that require higher energy for the initial steps in CO_2 reduction.

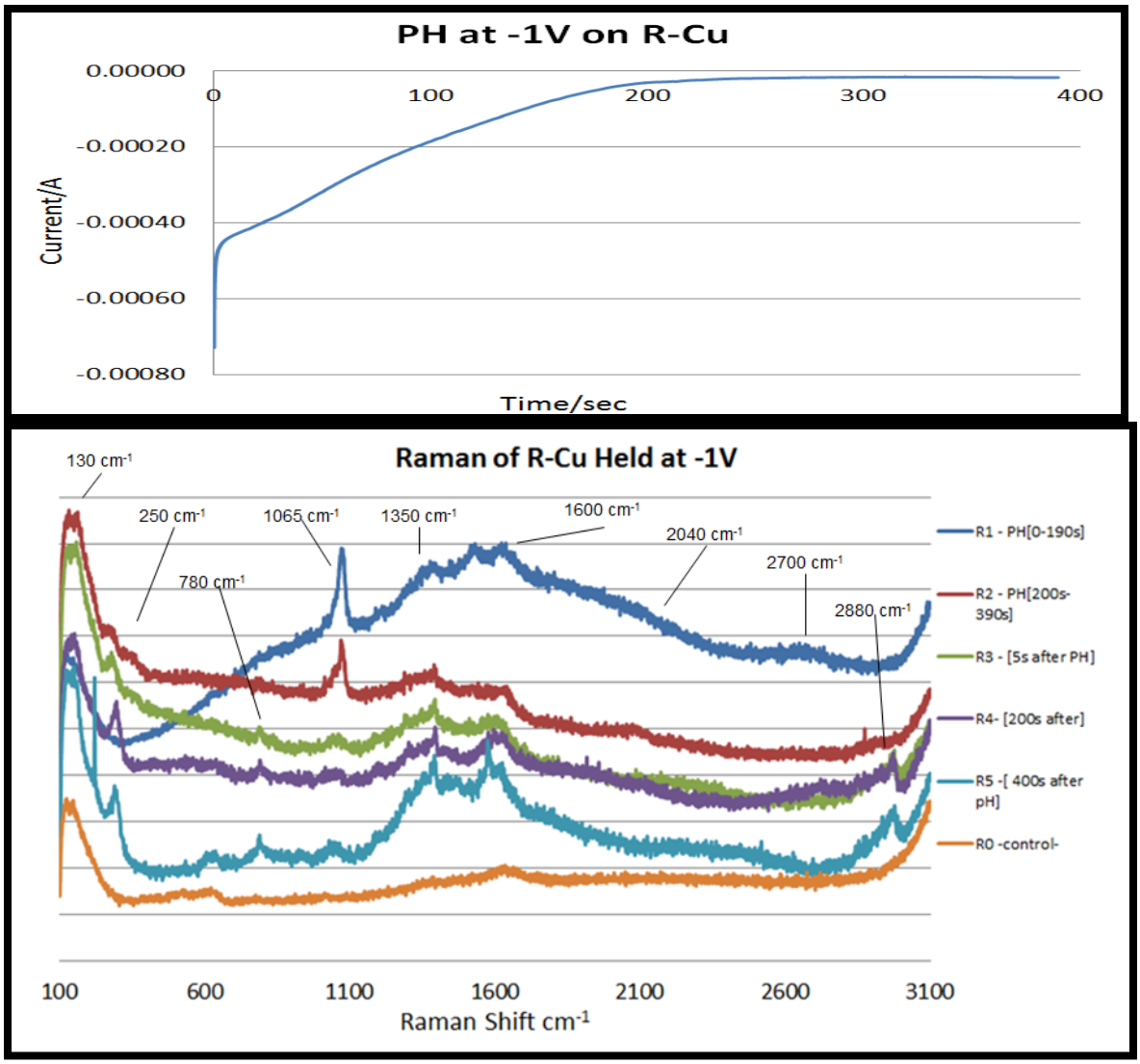

Figure 32: R-Cu potential hold (PH) at -1V for 390s (Top) and Raman of R-Cu CO_2 reduction during and after the PH (Bottom) also with R0 Raman control of R-Cu and CO_2 saturated solution with no potential applied.

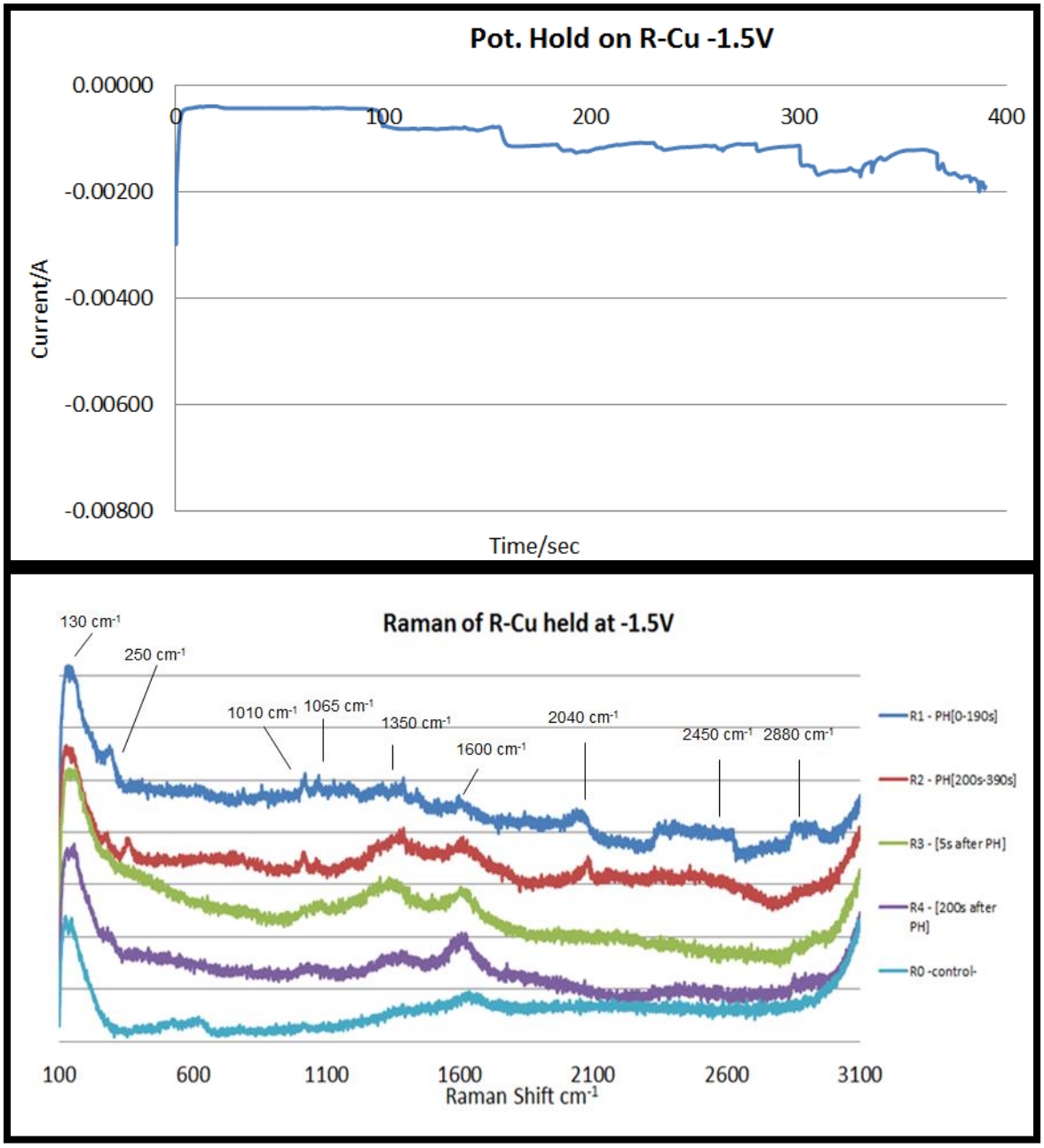

Figure 33: R-Cu potential hold (PH) at -1.5V for 390s (Top) and Raman of R-Cu CO_2 reduction during and after the PH (Bottom) also with R0 Raman control of R-Cu and CO_2 saturated solution with no potential applied.

The SERS spectra shown have many characteristic vibrational bands and these were used to explore the electrochemical reduction of CO_2 at a copper electrode in $KHCO_3$ aqueous solution saturated with CO_2 at room temperature [65]. We have identified many of the potential vibrational stretches and suggest some of their species that they correspond to (Table 2). The Raman scattering detected from the NpCu electrode suggests the formation of some copper oxide and more interestingly the formation of CO, $HCOO^-$ and hydrocarbons by CO_2 reduction [66,67]. For instance at a NpCu electrode held at a potential of -1 V (*vs.* Pt-pseudo RE), adsorbed CO gives rise to a C-O stretch band at 2040 cm^{-1} and adsorbed $HCOO^-$ or HCO_3^- species with C-OH and C-O stretches at 1010 and 1065 cm^{-1}. There is thought to be dual contribution from HCO_3^- and $HCOO^-$ to the 1010 and 1065 cm^{-1} vibrational bands due to the similarities between the two adsorbed species stretching, which adds to the vibrational intensity. It is observed that the bands of CO (2040 cm^{-1}) and $HCOO^-$ (1065 cm^{-1}) sharply increase then decrease in intensity as the potential hold is terminated and the cell returns to OCP or open circuit potential (Fig 34 Top). While, the largely HCO_3^- bands of 1350 and 1600 cm^{-1} remain relatively stable due to the flow and bubbled CO_2. Furthermore, when examining the peaks of NpCu held at -1.5V we see a similar trend of CO and $HCOO^-$ vibrational bands increasing then decreasing after the potential hold, however, it is also observed that hydrocarbon stretches trend opposite to that of the CO and $HCOO^-$ bands (Fig 34 bottom). The C-H stretch bands of 1410 and 2880 cm^{-1} only seem to increase after the peak in CO and $HCOO^-$ and after the potential hold is terminated. This is also observed on R-Cu where it seems the peak intensity's corresponding to CO and $HCOO^-$ are inversely related to those

of hydrocarbons (Fig 35). This suggest that CO and $HCOO^-$ could be the precursor species that are initially present on the surface, which then contribute to the production gaseous hydrocarbons. Then after the potential is terminated the gaseous hydrocarbon species are no longer bubble out of solution but reabsorb to the surface, and displacing most surface CO and $HCOO^-$ species. Though, the relationship between possible species and their upstream intermediates is promising this is still in the initial stages of characterization of the products and mechanisms involved with the reduction on copper catalyst. What is done here is provide a supposition based on the spectra and process, obtained on CO_2 reduction. We propose that CO and/or $HCOO^-$ produced from at lower potentials serve as surface precursors for hydrocarbon production and evolution. Moving forward we hope to utilize Raman more on standard chemicals along with GCMS, NMR, and other analytical techniques to further support or elucidate the process of what products are produced. Also, concerning the difficulty of collecting spectra due to gaseous species production new spectroeletrochemical flow cell design are being considered and tested with and emersion objective.

Raman Shift (cm^{-1})	Band Assignment	Possible Species on Cu
110- 130	Potential Cu_2-O	
250	Cu-O or Cu-OH	Cu-oxide
545	Potential Cu-O	
630	V_7 C-O bend	HCO_3^-
780	Potential C-O	CO_3^{2-}
1010	V_5 C-OH	$HCOO^-$ or $\underline{HCO_3^-}$
1065	V_1 C-O	$\underline{HCOO^-}$ or HCO_3^-
1210	Potential C-O or C-C	HCO_3^-
1350	V_3 O-C-O	HCO_3^-
1410	Potential C-H	Hydrocarbons
1600	O-H or O-C-O	$\underline{HCOO^-}$ or HCO_3^-
1770	Unassigned	
2040	C-O	CO
2450-2700	V_1 O-H or C-H	$\underline{HCOO^-}$ or HCO_3^-
2830	Potential C-H	$HCOO^-$
2880	Potential C-H	Hydrocarbons

Table 2: Peak assignment for potential surface species present on NpCu and R-Cu [65,66,67]. The underlined species predominate with some contribution at time from a similar species.

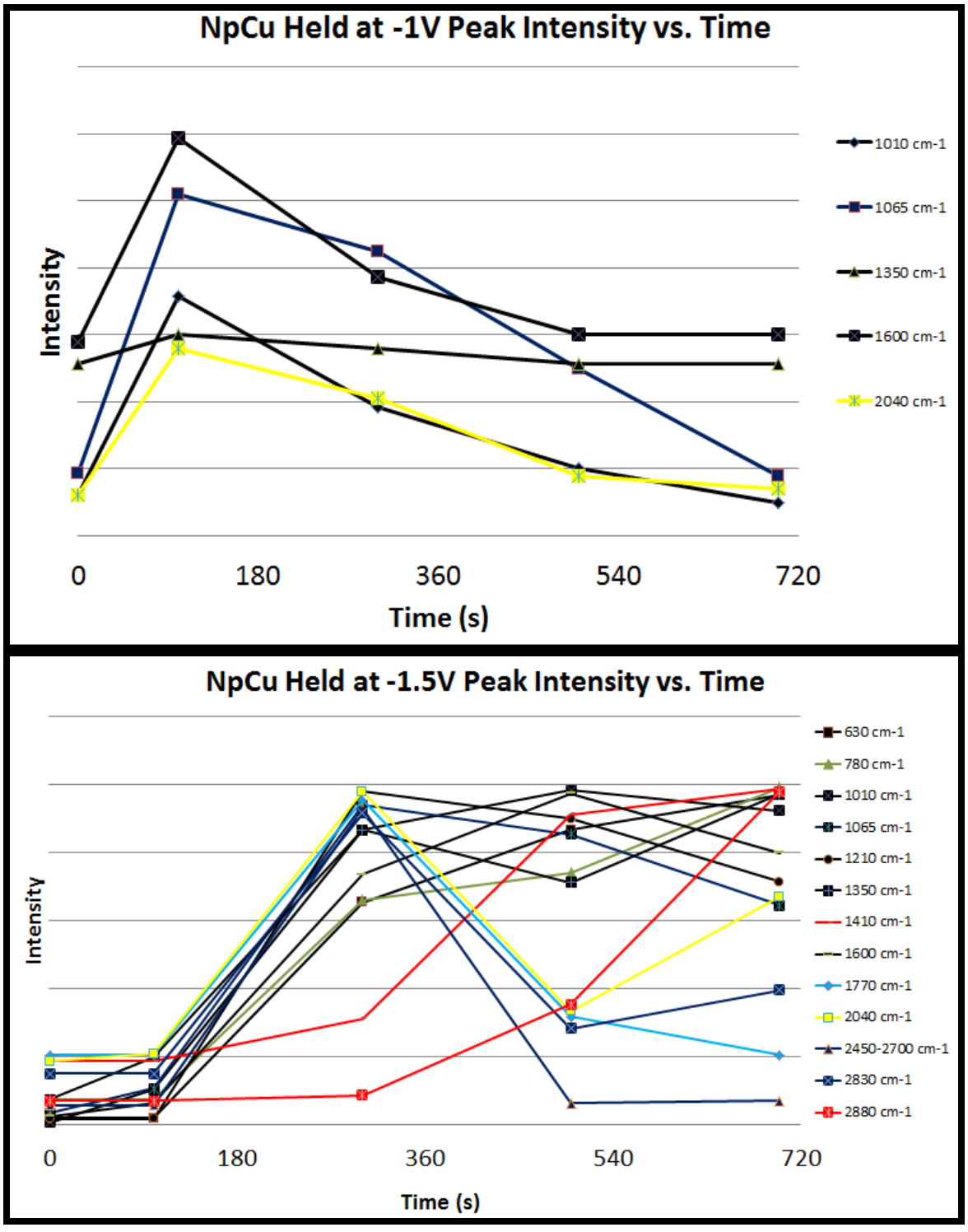

Figure 34: Chart of NpCu Peak Intensities while held at -1V (top) and -1.5V (bottom) for around 400 seconds. The line colors correspond to the predominant species of the vibrational band. Black (HCO_3^-), Blue ($HCOO^-$), Yellow (CO), Red (Hydrocarbons), Green (CO_3^{2-}) and Light blue (unassigned).

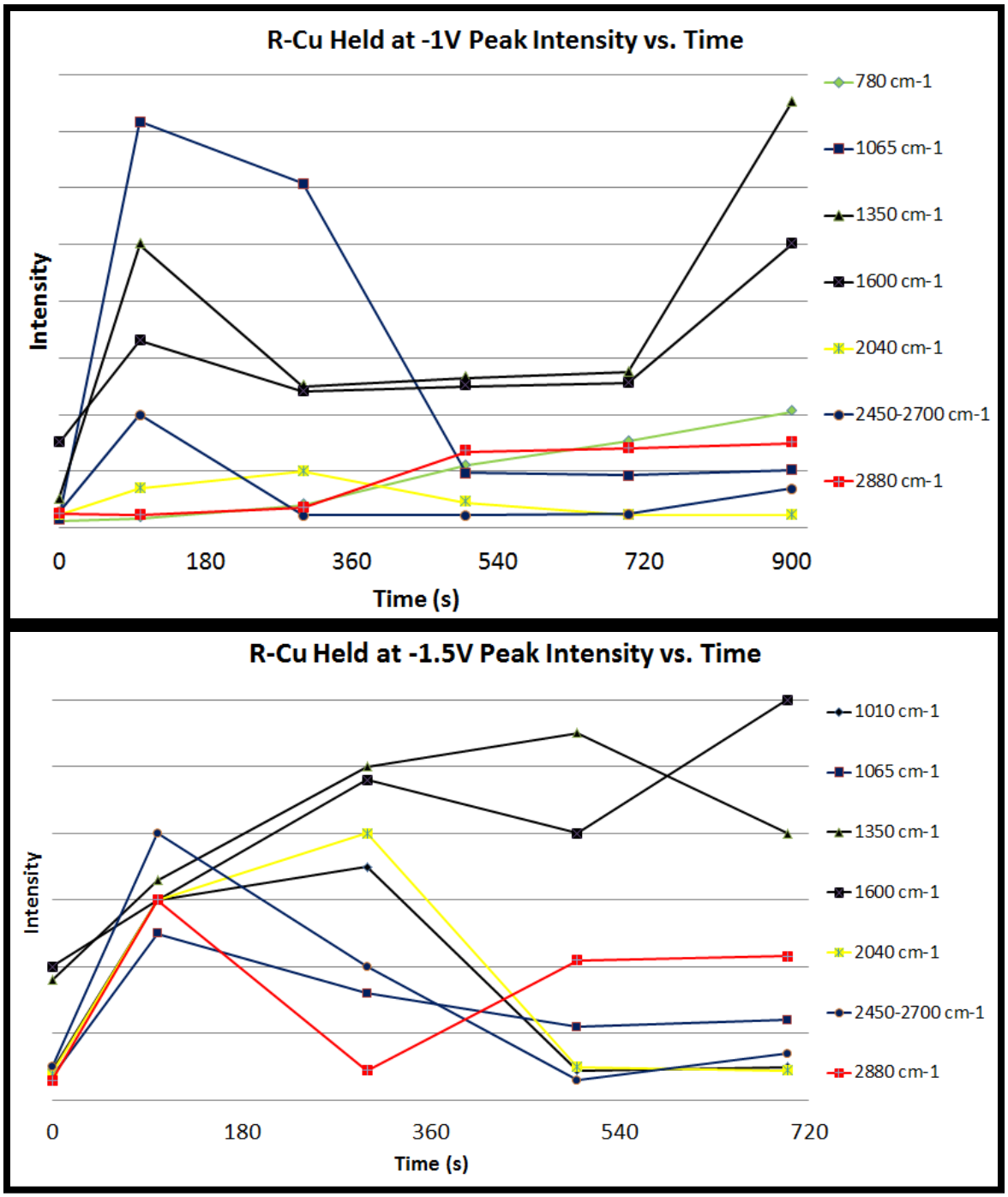

Figure 35: Chart of R-Cu Peak Intensities while held at -1V (top) and -1.5V (bottom) for 400 seconds. The line colors correspond to the predominant species of the vibrational band. Black (HCO_3^-), Blue ($HCOO^-$), Yellow (CO), and Red (Hydrocarbons).

6 Summary

The turn of the 21st century brought about a harsh realization that society would not be able to maintain its hunger for energy and resources while relying on fossil fuel combustion and produce environmentally harmful greenhouse gases (GHGs), namely CO_2. As a results many alternative energy technologies have been introduced, however petrol chemical combustion dominate the energy supply of most sectors, and CO_2 levels continue to rise rapidly. Thus methods of CO_2 recycling and utilization will need to be developed for the mitigation of climate change due to increased GHGs. Electrochemical reduction is an attractive method for converting CO_2 to products that have potential use as fuel or feedstock currently consumed in our present infrastructure but mechanistic information is required to increase the efficacy to the process. For my project, using promising copper based catalyst for electroreduction and vibrational spectroscopy like Raman, are valid tools for intermediate detection. Optimized SERS was be employed to increase likelihood of detecting low concentration intermediates, thus we made and optimized the SERS catalyst nanoporous copper (NpCu) and found the optimum SERS pore size is around 500 nm. We have begun to reduce saturated CO_2 solution on the SERS copper catalyst and detected a multiple vibrational bands and found that CO and $HCOO^-$ may be precursor species/ intermediates on at the copper surface that are converted into hydrocarbon at high potentials. Also, further testing and data can be employed for increased knowledge on this highly promising work.

7 References

1. Barker T. I. B., Bernstein, L.; Bogner, J. E.; Bosch, P. R.; Dave, R.; Davidson, O. R.; Fisher, B. S.; Gupta, S.; Halsnæs, K.; Heij,G. J.; Kahn Ribeiro, S.; Kobayashi, S.; Levine, M. D.; Martino, D. L.; Masera,O.; Metz, B.;Meyer, L. A.; Nabuurs, G.-J.; Najam,A.; Nakicenovic, N.; Rogner, H.-H.; Roy, J.; Sathaye, J.; Schock, R.; Shukla, P.; Sims, R. E. H.; Smith, P.; Tirpak, D. A.; Urge-Vorsatz, D.; Zhou, D. IPCC, 2007: Climate Change 2007: Mitigation. Contribution of Working Group III to the Fourth Assessment Report of the Intergovernmental Panel on Climate Change;Metz, B., Davidson,O.R., Bosch, P. R.,Dave, R.,Meyer,
2. IPCC**,** 1991: The First Assessment Report of the Intergovernmental Panelon Climate Change (IPCC). Cambridge University Press, Cambridge.
3. Rijsberman**,** F.J., and R.J. Swart (eds.), 1990: Targets and Indicators of climate Change. Stockholm Environment Institute, 1666 pp.
4. Baker**,** T., H. Pan, J. Kohler, R. Warren, and S. Winne, 2006: Avoiding Dangerous Climate Change by Inducing Technological Progress: Scenarios Using a Large-Scale Econometric Model. In *Avoiding Dangerous Climate Change*, H.J. Schellnhuber (editor in chief), Cambridge University Press, pp. 361-371.
5. Bolin**,** B. and H.S. Kheshgi, 2001: On strategies for reducing greenhouse gas emissions. Proceedings of the National Academy of Sciences ofthe United States of America, 24 April, 2001, **98**(9), pp. 4850-4854.
6. EIA**,** 2006a: U.S. Department of Energy, Energy InformationAdministration, Washington, D.C., 20585, http://www.eia.doe.gov/meu/international/crude1.html>, accessed 15. December 2012.
7. Olivier**,** J.G.J., J.A. Van Aardenne, F. Dentener, V. Pagliari, L.N. Ganzeveld, and J.A.H.W. Peters, 2005: Recent trends in global greenhouse gas emissions: regional trends 1970-2000 and spatial distribution of key sources in 2000. *Environmental Science*, **2**(2-3), pp. 81-99. DOI: 10.1080/15693430500400345. <http://www.mnp.nl/edgar/global_ overview/>, accessed 15. December 2012.
8. IPCC**,** 1996: The Second Assessment Report of the Intergovernmental Panel on Climate Change (IPCC). Cambridge University Press, Cambridge.
9. IPCC**,** 2000a: Emissions Scenarios. [Nakicenovic, N. and R. Swart (eds.)]. Special Report of the Intergovernmental Panel on Climate Change(IPCC). Cambridge University Press, Cambridge, 570 pp.
10. UN**,** 1992: United Nations Framework Convention on Climate Change,United Nations, New York.
11. Bernstein L, et al**.** Climate change 2007: synthesis report; an assessment of the IPCC 2007: pp 9 http://www.ipcc.ch/publications_and_data/ar4/wg1/en/faq-3-1-figure-1.html. Accessed 22 November 2012.
12. Kaya**,** Y, 1990: Impact of Carbon Dioxide Emission Control on GNP Growth: Interpretation of Proposed Scenarios. Paper presented to the IPCC Energy and Industry Subgroup, Response Strategies Working Group, Paris.
13. Bernstein L, et al**.** Climate change 2007: synthesis report; an assessment of the IPCC 2007: pp 10 http://www.ipcc.ch/publications_and_data/ar4/wg1/en/faq-3-1-figure-1.html. Accessed 22 November 2012.
14. Mastrandrea**,** M.D., and S.H. Schneider, 2004: Probabilistic Integrated Assessment of 'Dangerous' Climate Change. *Science*, 304(5670), pp.571-575.
15. Van der Werf**,** G.R., J.T. Randerson, G.J. Collatz, and L. Giglio, 2003:Carbon emissions from fires in tropical and subtropical ecosystems. *Global Change Biology*, **9**, pp. 547-562.
16. Marland**,** G., T.A. Boden, and R.J. Andres, 2006: Global, Regional, and National Fossil Fuel CO2 Emissions. In *Trends: A Compendium of Data on Global Change.* Carbon Dioxide Information Analysis Center, Oak Ridge National Laboratory, U.S. Department of Energy, Oak Ridge, Tenn., USA.
17. Bernstein L, et al**.** Climate change 2007: synthesis report; an assessment of the IPCC 2007: pp 14 http://www.ipcc.ch/publications_and_data/ar4/wg1/en/faq-3-1-figure-1.html. Accessed 22 November 2012.
18. Bernstein L, et al**.** Climate change 2007: synthesis report; an assessment of the IPCC 2007: pp 16 http://www.ipcc.ch/publications_and_data/ar4/wg1/en/faq-3-1-figure-1.html. Accessed 22 November 2012.
19. Sun**,** J.W., 1998: Changes in energy consumption and energy intensity:A complete decomposition model. *Energy Economics* **20**(1), pp. 85-100.
20. Bernstein L, et al**.** Climate change 2007: synthesis report; an assessment of the IPCC 2007: pp 4 http://www.ipcc.ch/publications_and_data/ar4/wg1/en/faq-3-1-figure-1.html. Accessed 22 November 2012.
21. Ramankutty**,** N., *et al*., 2006: Challenges to estimating carbon emissions from tropical deforestation. *Global Change Biology* (published article).
22. Nordhaus**,** W.D., 2006: The *Stern Review* on the Economics of ClimateChange. National Bureau of Economic Research, Working Paper 12741. Cambridge, Massachusetts, USA.
23. Olivier**,** J.G.J., J.A. Van Aardenne, F. Dentener, V. Pagliari, L.N. Ganzeveld,and J.A.H.W. Peters, 2005: Recent trends in global greenhouse gas emissions: regional trends 1970-2000 and spatial distribution of key

sources in 2000. *Environmental Science*, **2**(2-3), pp. 81-99. DOI:10.1080/15693430500400345. <http://www.mnp.nl/edgar/global_overview/>, accessed 5. December 2006.
24. Olivier**,** J.G.J., T. Pulles and J.A. van Aardenne, 2006: Part III: Greenhouse gas emissions: 1. Shares and trends in greenhouse gas emissions; 2. Sources and Methods; Greenhouse gas emissions for 1990, 1995 and 2000. In *CO2 emissions from fuel combustion 1971-2004*, 2006 Edition, pp. III.1-III.41. International Energy Agency (IEA), Paris. ISBN 92-64-10891-2 (paper) 92-64-02766-1 (CD ROM) (2006).
25. Pacala**,** S. and R. Socolow, 2004: Stabilization Wedges: Solving the Climate Problem for the Next 50 Years with Current Technologies.*Science*, **305**, pp. 968-972.
26. Annual Energy Review2008; U.S. Energy Information Agency: Washington, DC, 2009.
27. Share of Total Energy Consumption by Fuel in 2007. European Environment Agency; http://www.eea.europa.eu/data-andmaps/ figures/share-of-total-energy-consumption (2010).
28. F Lee, B. S.; Gushee, D. E. Electricity Storage: The Achilles' Heel of Renewable Energy. Chem. Eng. Prog. 2008, 104, S29–S32.
29. Annual Energy Outlook 2010 with Projections to 2035; U.S. Energy Information Agency: Washington, DC, 2010.
30. Sanchez-Sanchez, C. M.; Montiel, V.; Tryk, D. A.; Aldaz, A.;Fujishima, A. Electrochemical Approaches to Alleviation of the Problem of Carbon Dioxide Accumulation. Pure Appl. Chem. 2001, 73, 1917–1927.
31. Choi, S.; Drese, J. H.; Jones, C. W. Adsorbent Materials for Carbon Dioxide Capture from Large Anthropogenic Point
Sources. ChemSusChem 2009, 2, 796–854.(5) Hao, X.; Djatmiko, M. E.; Xu, Y. Y.; Wang, Y. N.; Chang, J.; Li, Y.W. Simulation Analysis of a GTL Process Using ASPEN Plus. Chem. Eng. Technol. 2008, 31, 188–196.
32. Sudiro, M.; Bertucco, A. Production of Synthetic Gasoline and Diesel Fuel by Alternative Processes Using Natural Gas and
Coal: Process Simulation and Optimization. Energy 2009, 34, 2206–2214.
33. Sudiro, M.; Bertucco, A.; Ruggeri, F.; Fontana, A. Improving Process Performances in CoalGasification for Power and SynfuelProduction. Energy Fuels 2008, 22, 3894–3901.
34. Turner, J.; Sverdrup, G.; Mann, M. K.; Maness, P. C.; Kroposki, B.; Ghirardi, M.; Evans, R. J.; Blake, D. Renewable Hydrogen Production. Int. J. Energy Res. 2008, 32, 379–407.
35. Langhamer, O.; Haikonen, K.; Sundberg, J. Wave Power- Sustainable Energy or Environmentally Costly? A Review with Special Emphasis on LinearWave Energy Converters. Renewable Sustainable Energy Rev. 2010, 14, 1329–1335.
36. Lenzen, M. Current State of Development of Electricity- Generating Technologies: A Literature Review. Energies 2010, 3, 462–591.
37. World Bank**,** 2006: Clean energy and development: towards an investment framework. Environmental and Socially Sustainable Development Vice Presidency, World Bank, Washington D.C., March.
38. Annual Energy Review2008; U.S. Energy Information Agency: pp. 36 Washington, DC, 2009.
39. Vallette**,** J. and D. Wysham, 2002: Enron's pawns - how public institutions bankrolled Enron's globalization game. Sustainable Energy and Economy Network, Institute of Policy Studies, Washington D.C.
40. Vate**,** J.F. van de, 2002: Full-energy-chain greenhouse-gas emissions: a comparison between nuclear power, hydropower, solar power and wind power. *International Journal of Risk Assessment and Management 2002*, **3**(1), pp. 59-74.
41. F Lee, B. S.; Gushee, D. E. Electricity Storage: The Achilles' Heel of Renewable Energy. Chem. Eng. Prog. 2008, 104, S29–S32.
42. Kenis, P; D. Whipple; Prospects of CO2 Utilization via Direct Heterogeneous Electrochemical Reduction. DOI: 10.1021/jz1012627 |J. Phys. Chem. Lett. 2010, 1, 3451–3458
43. Hori, Y.;Wakebe, H.; Tsukamoto, T.; Koga, O. ElectrocatalyticProcess of CO Selectivity in Electrochemical Reduction of CO2 at Metal-Electrodes in Aqueous-Media. Electrochim. Acta1994, 39, 1833–1839.
44. Hori, Y.;Wakebe, H.; Tsukamoto, T.; Koga, O. 25 years of Electrochemistry, Electrocatalytic Process of CO Selectivity in Electrochemical Reduction of CO2 at Metal-Electrodes in Aqueous-Media. Electrochim. Acta1994, 39, 1833–1839.
45. Gattrell, M, Gupta N, Co A. Electrochemical reduction of CO2 to hydrocarbons to store renewable electrical energy and upgrade biogas. Energy Conversion and Management 48 (2007) 1255–1265
46. Hori Y, Murata A, Takahashi R. Formation of hydrocarbons in the electrochemical reduction of carbon dioxide at a copper electrode in aqueous solution. J Chem Soc, Faraday Trans 1 1989;85(8):2309–26.
47. Hara K, Tsuneto A, Kudo A, Sakata T. Electrochemical reduction of CO2 on a Cu electrode under high pressure. J Electrochem Soc 1994;141(8):2097–103.
48. Gattrell M, Gupta N, Co A. A review of the aqueous electrochemical reduction of CO2 to hydrocarbons at copper. J Electroanal Chem 2006;594:1–19.
49. G. Venkataraman, 'Journey into light: life and science of C. V. Raman,' Indian Academy of Science, 1988.
50. S.A. Maier, Plasmonics: Fundamentals and Applications, Springer (2007).

51. C.F. Bohren and D.R. Huffman, Absorption and Scattering of Light by Small Particles, Wiley, New York (1983).
52. Fleischmann, M., *et al., Chem Phys Lett* (1974) **26**, 163.
53. Jeanmai re, D. L., and Van Duyne, R. P., *J Electroanal Chem* (1977) **84**(1), 1
54. Moskovits M (1985) Rev Mod Phys 57:783–826
55. Kerker M (1984) Acc Chem Res 17:271–277
56. Otto A, Mrozek I, Grabhorn H, Akemann W (1992) J Phys Condens Matter 4:1143–1212
57. Lombardi JR, Birke RL, Lu TH, Xu J (1986) J Chem Phys84:4174–4180
58. Ren B, Liu GK, Lian, XB, Yang ZL, Tian ZQ; Raman spectroscopy on transition metals; Review 2007
59. Sharma, B., Fontiera, R., Henry A., Ringe, E., and Van Duyne, R. P., *SERS: Material and Applications for the future* (2012), Materials Today Review **15**(16-25)
60. Van Duyne, R. P. et al. Nanosphere lithography: Tunable localized surface plasmon resonance spectra of silver nanoparticles. *J. Phys. Chem. B* 2000
61. Dolata, M. et al. Characterization of the copper surface optimized for use as a substrate for surface-enhanced Raman scattering. Vib Spec 16 1998. 21–29
62. Gaff J., S. Franzen; Resonance Raman enhancement of pyridine on Ag clusters. Chem. Phys 397, 2012, 34-41
63. Camden J.,J. Dieringer, J. Zhao, R. P. Van Duyne; Controlled Plasmonic Nanostructures for Surfaced-Enhanced Spectroscopy and Sensing; Acc. of Chem. Res., 2008, 41, 12, 1653-1661
64. Yang L, Yu JS, Fujita T, Chen W; Nanoporous Copper with Tunable Nanoporosity for SERS Applications Adv. Funct. Mater. 2009, 19, 1221–1226
65. Ichinohe, Y., Wadayama, T., and Hatta, A., Electrochemical Reduction of C02 on Silver as Probed by Surface-Enhanced Raman Scattering (1995), J, OF RAMAN SPEC, VOL. 26, 335-340
66. S.M. Williams, K.R. Rodriguez, S. Teeters-Kennedy, A.D. Stafford, S.R. Bishop,U.K. Lincoln, and J.V. Coe, Using the extraordinary infrared transmission of metallic subwavelength arrays to study the catalyzed reaction of methanol to formaldehyde on copper oxide., J. Phys. Chem. B, **108** 11833-11837 (2004).
67. B. D. Smith; PhD Thesis: A SERS Study of the Electrochemical Reduction of Carbon Dioxide on Copper Electrodes. University of Waterloo, Canada. 1998.